MIXING OF GRANULAR MATERIALS IN AN OSCILLATORY SHEAR MIXER

by

Luis Guillermo Obregón Quiñones

A thesis submitted in partial fulfillment of the requirements for the degree of

DOCTOR OF PHILOSOPHY
in
CHEMICAL ENGINEERING

UNIVERSITY OF PUERTO RICO
MAYAGÜEZ CAMPUS
2009

Approved by:

Carlos Velázquez Figueroa, Ph.D.
President, Graduate Committee
Date

David Suleiman Rosado, Ph.D.
Member, Graduate Committee
Date

Carlos Rinaldi, Ph.D.
Member, Graduate Committee
Date

Jaime Benítez, Ph.D.
Member, Graduate Committee
Date

Rodolfo Romañach Suárez, Ph.D.
Representative of Graduate Studies
Date

David Suleiman Rosado, Ph.D.
Chairperson of the Department
Date

ABSTRACT

Mixing is one of the most important steps in handling powders in many industries e.g., the chemical, metallurgical, pharmaceutical, and food processing industries, because it strongly affects the composition of their main products. To mention only one important example in the pharmaceutical industry, mixing affects the potency of tablets such that if a problem of non homogeneity in its components results, it becomes a risk to human health.

To obtain an in depth understanding of mixing behavior, most previous studies have been emphasized in different systems such as rotating cylinders, tote blenders, v-blenders, double cone blenders, etc which are the most used nowadays in industries of solid handling. The progress has been substantial, however, because of the fact that most of the work has been done regarding only 2 dimensions, fundamental comprehension of the phenomena is still hidden. Real industrial applications require the understanding in three dimensions and only few studies along these lines has been done, for example, the use of new techniques such as positron emission particle tracking (PEPT) which is a noninvasive method that follows the motion of single radioactively labeled tracer particle to study their displacement in three axes. The use of MRI is another not so common technique in this field and the reason of the limitation of the use of these equipments is the high costs involved, and the complexity to have them in a common laboratory.

Considering the limitations and complications experienced in the general study of granular mixing, this work focused on developing a simple system consisting of a box with two moving walls and three static walls where the imposed shear strain was varied following a periodic function which permits to study the granular material's random movement and the mixing of the granular material.

The goal was to demonstrate experimentally, with a relatively simple system, the importance of taking into consideration the three dimensions and to obtain insights of the

physical phenomena (compaction, dilation, interface slip, chaos, and segregation) involved in 3-dimensional granular flow. The system allows targeting specific phenomena, thus better understanding can be drawn from the experimental results.

The results are explained in three chapters. In the first, the effect of experiments at different imposed shear strains, wall displacements, time, and wall perturbation in the mixing on the surface of the cavity and in the z-axis were studied. Segregation was another phenomenon considered to understand the diverse responses of the mixing in the system when problems of non-homogeneity appear. In the second chapter the effects of different particle size distributions and dilation are shown. Finally, the third chapter concerns the effect of initial filling level in global mixing.

The study reveals that the best mixing is found near the moving walls and in the superficial layer. A triangular pattern with a height decrease that is associated with an increase in mixing was obtained at the bottom of the mixing chamber. The triangle size depended on the length of the mixing chamber, the velocity and wall displacement, the particle size, and the initial filling level. Mixing in the superficial layer follows a chaotic trend. The phenomenon of dilation was significant, playing an important role in the mixing performance varying the expansion of the bed linearly with the particle size.

RESUMEN

Mezclado es uno de los pasos mas importantes en el manejo de los polvos en muchas industrias tales como en la industria química, metalúrgica, farmacéutica, alimenticia, etc., debido al gran efecto que tiene en la composición de sus productos principales. Para mencionar solo un importante ejemplo en la industria farmacéutica, el mezclado afecta altamente la potencia de las tabletas de tal manera que si hay un problema de no homogeneidad en sus componentes, esto se convertiría en un gran riesgo a la salud humana.

Para ir más a fondo en el entendimiento del comportamiento del mezclado, la mayoría de los estudios han sido enfatizados en diferentes sistemas tal como cilindros rotatorios, mezcladores tote, mezcladores en V, mezcladores de doble cono, etc., los cuales son los más usados hoy en día en la industria del manejo de sólidos. El progreso ha sido substancial, aunque, debido al hecho de que la mayoría del trabajo haya sido realizado considerando solo en 2 dimensiones, la comprensión fundamental de los fenómenos permanece aun oculta. Las aplicaciones reales de la industria requieren el entendimiento en las tres dimensiones y solo pocos estudios en esta línea ha sido realizados, por ejemplo, el uso de nuevas técnicas tales como el rastreo de partículas por emisión de positrones la cual es una técnica no invasiva que sigue el movimiento de partículas trazadoras marcadas radiactivamente para estudiar su desplazamiento en los tres ejes coordenados. El uso de MRI es otro método no muy común en este campo y la razón del poco uso de estos equipos es debido al alto costo envuelto y la complejidad y dificultad de tenerlos en un laboratorio común.

Considerando las limitaciones y complicaciones experimentadas por el estudio general acerca del mezclado granular, este trabajo ha sido enfocado en desarrollar un sistema simple que consiste de una caja que tiene dos paredes movibles y tres paredes estáticas donde la deformación cortante impuesta fue variada siguiendo una función periódica la cual permite el estudio del movimiento aleatorio del material granular y el mezclado de este.

El objetivo fue demostrar experimentalmente con un sistema no complicado la relevancia de la importancia de tomar en consideración una tercera dimensión y conseguir información de los fenómenos físicos (compactación, dilatación, deslizamiento de interfase, caos, y segregación) envueltos en el flujo granular de tres dimensiones. El sistema permite enfocar fenómenos específicos y así un mejor entendimiento de estos puede ser obtenido de resultados experimentales.

Los resultados son explicados en tres diferentes capítulos principales. En el primero de ellos, el efecto de los experimentos a diferente deformación cortante impuesta, desplazamientos de pared, tiempo y perturbación de pared en el mezclado de la superficie de la cavidad y en el eje z fueron estudiados. Segregación fue otro fenómeno considerado para entender las respuestas diversas de mezclado en el sistema cuando problemas de no homogeneidad aparecen.

En el segundo capitulo los efectos de diferentes distribuciones de tamaño de partícula y dilatación son mostrados. Por ultimo, el tercer capitulo concierne al efecto de nivel de llenado inicial en el mezclado global.

El estudio revela que el mejor mezclado es encontrado cerca de las paredes movibles y en la capa superficial. Un patrón triangular con una altura decreciente asociada con el incremento del mezclado fue obtenido en el fondo de la cámara de mezclado y cuya longitud depende del largo de la cavidad, la velocidad, el desplazamiento de la pared, el tamaño de partícula y el nivel de llenado inicial. El mezclado en la capa superficial sigue un comportamiento caótico. El fenómeno de dilatación fue notable jugando un papel importante en el desarrollo del mezclado variando la expansión del lecho linealmente con el tamaño de partícula.

To my almighty and merciful Lord
Jesus Christ

To my most loved ones
My wife Norleyn, My beautiful daughter Valerie,
My mom Mirtala, My father William, My aunt Daysi
and My brothers Aníbal, William, and José.

ACKNOWLEDGEMENTS

First of all, I wish to thank Dr. Carlos Velázquez, my advisor, for being not only an excellent guide but also an excellent friend during all these years of study. He always trusted on my capabilities encouraging me with great enthusiasm to give the best of my potential to go in deep in a new field of research for this university as is the flow and mixing of granular materials.

I wish to acknowledge the University of Puerto Rico at Mayagüez campus and the Chemical Engineering Department for giving me the majority of financial support to develop this research project, which allows me to pursue my PhD degree.

I am thankful to the other three members of my thesis committee, Dr. Carlos Rinaldi, Dr. David Suleiman, and Dr. Jaime Benitez for their valuable contributions to accomplish my objectives.

I want to thank Dr. Alvaro Realpe for sharing his experience and knowledge in the laboratory pharmaceutical engineering.

I want to express my sincere gratitude to Dr. Carlos Ramírez, Dr. David González, Dr. Moses Bogere, Dr. Nelson Cardona, Dr. Julio Briano, Dr. Lorenzo Saliceti, Dr. Frederick Just, and Dr. Fernando Muzzio for their important contributions to my professional growth.

I would also want to express my gratefulness to Mr. Angel Zapata for his great help on troubleshooting the laboratory equipment. I am so pleased that I have no words to thank all the people who became part of my life and encouraged me to keep on doing the best during all this years of study.

This work was supported partially by the Engineering Research Center for Structured Organic Particulate Systems (ERC-SOPS)

Table of Contents

Table List

Tables **Page**

Figure List

Figures **Page**

1 INTRODUCTION

There still exists a great deal of interest in understanding concentrated granular flow, which is a flow having two phases consisting of particulates and an interstitial fluid [1, 2]. This is a very important phenomenon for processes in industries such as pharmaceutical, chemical, metallurgical, building materials, power, textile, environmental protection, agriculture, and food industry, etc., [1, 3-11]. Granular flow can be seen in mechanical unit operations for instance in a coal or flour flow in a silo, powder flowing by gravity in a hopper, and flow of mixtures of fertilizers or pharmaceutical powders in a tumbling blender [4, 12-21].

The significance of granular flow affects as well the area of simple storage of powders [12, 22], which is one of the areas where the industry has obtained the larger economic losses due to irregular failure in the design of hoppers, silos, and huge storage containers [23]. Besides storage and strictly speaking granular flow, another problem of high importance is the achievement of homogeneous mixtures of powders in the pharmaceutical industry to comply with the stringent specifications of the FDA in the production of tablets to avoid under or overdose [8, 9].

The comprehension of the above mentioned processes involves much information on material properties of coarse solids [24], concentration tendencies [25], and pre-stressing [26] history. These are a few examples of the importance of flow and mixing of granular materials, which are less understood than fluid mixing and, in contrast, there is no agreement on the starting point regarding the fundamental equations [27, 28].

1.1 Granular flow

Granular flow is a phenomenon described by three regimes, Fig. 1, depending on the type of collisions of the particles [20, 29-34]. The first regime where particles arbitrarily oscillate and translate is the dilute phase, this form of viscous dissipation and stress is named kinetic [23]. In the second regime, which is at higher concentration of grains, particles cascade over each other interacting by short collisions [35], giving rise to further energy dissipation and stress due to the surface inelasticity. This regime is called kinetic collisional.

The combination of the two mentioned regimes is called rapid flow. The flow behavior of cohesionless materials in the rapid regime has received significant attention in many prior studies [31, 36-50]. In these works, the flow has been studied using statistical approach making analogies with the kinetic theory of dense gas.

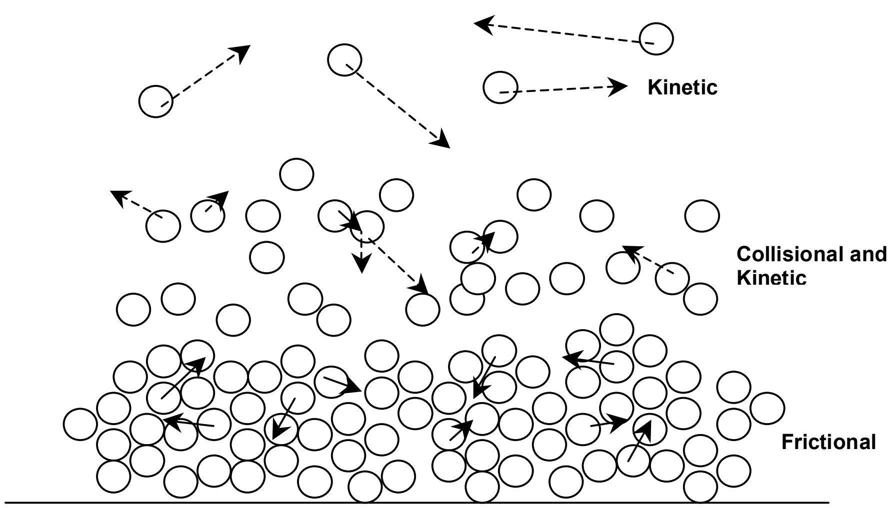

Fig. 1. The three major types of viscous dissipation within a granular flow: kinetic - kinetic and collisional - frictional

In the third regime, which is at very high concentration of particles, higher than 50% in volume [23], the overwhelming interaction between individual particles is considered surface friction during which particles slide on top of each other [35] increasing the frictional dissipation [23]. This regime is called slow flow and is generally modeled using basic concepts of soil mechanics based on the well known yield hypothesis of Mohr and Coulomb by means of the theory of plasticity [23, 51-54]. This theory describes materials such as ductile metals, clay, and putty, which have the property of changing their shape easily by the application of appropriately directed forces, and retain their new shape upon removal of such forces.

The above mentioned regimes have been applied by many authors to different mixers [16-21], and different and complicated configurations, operating conditions, and powder properties. Limited results have been obtained due to the many restrictions applied compared to the large number of factors necessary to describe the real behavior and to understand each one of the phenomena happening in powder flow.

Other researchers have used or use continuum mechanics to predict the behavior of powder flow [23, 33, 35, 48, 52, 55-57]. The aim of these simulations is to obtain the necessary and sufficient conditions that lead to the best mixing. The typical approach in the simulations is the use of constitutive relations that relate the frictional stress tensor to the rates of deformation. This relation is then substituted in the momentum balance Eq. (9) to finally obtain, with the use of mass balance Eq. (10), the velocity profiles of the powder and the location of particles in the bulk. Most of the constitutive equations used are similar to the general Newtonian constitutive equation for viscous stress in liquids. Some examples are shown in Eq. (1) [20], Eq. (2) [58] and Eq. (3) [59].

$$T = PI - \left(\frac{\tau_0}{|D|} + \mu \frac{\tau_0}{|D|} + \mu \right) D \qquad \textbf{(1)}$$

$$T = PI - \sqrt{2} P \sin\varphi \frac{D}{|D|} \qquad \textbf{(2)}$$

$$T = C_0 \varepsilon I - \frac{C_1 \varepsilon (1+\varepsilon)}{2} D \quad \textbf{(3)}$$

T is the stress tensor, D is the shear rate of strain or rate of deformation, I is the unit tensor, τ_0 is the constant yield strength which makes the powders to satisfy the yield condition (a linear law between the shear stress and the normal stress to produce the shearing), μ is the shear viscosity, P is the hydrostatic pressure, ε is the porosity, and C_1 and C_0 are parameters that depend on the characteristic of the system. Equations 1, 2, and 3 do not take in to account the volumetric rate of strain (compression / extension), an important factor for powders which have porosity and thus exhibit consolidation and dilatation.

On the other hand, Eq. (4) and Eq. (5) are constitutive equations that indeed consider the volumetric rate of strain and consequently have the capacity to give better flow predictions [23, 24]. In Eq. (4), ρ is the bulk density of the material, $\beta_0(\rho)$ plays the function analogous to pressure in a compressible fluid, $\beta_1(\rho)$ and $\beta_4(\rho)$ are material parameters that reflect the distribution of the granular solids, $\beta_3(\rho)$ denotes the shear viscosity, $\beta_2(\rho)$ is the corresponding term to the second coefficient of viscosity, and $\beta_5(\rho)$ is the cross viscosity which is related to the relaxation time. In Eq. (5), μ^s and μ^b are the shear (Eq. 6) and dilatational (Eq. 7) viscosities respectively, φ is the angle of internal friction, and II_{dD} is the second invariant of the deviator of the stress tensor. The symbol ⊗ refers to the dyadic product.

$$T = [\beta_0 + \beta_1(\rho)\nabla\rho\cdot\nabla\rho + \beta_2(\rho)trD]I + \beta_3(\rho)D + \beta_4(\rho,\nabla\rho)\nabla\rho\otimes\nabla\rho + \beta_5(\rho)D^2 \quad \textbf{(4)}$$

$$T = PI + \mu^b\nabla\cdot vI - 2\mu^S D \quad \textbf{(5)}$$

$$\mu^S = \frac{P\sin^2\phi}{\sqrt{4II_{dD}\sin^2\phi + (\nabla\cdot v)^2}} \quad \textbf{(6)}$$

$$\mu^b = \frac{P}{\sqrt{4II_{dD}\sin^2\phi + (\nabla\cdot v)^2}} \qquad \textbf{(7)}$$

$$D_{ij} = \frac{1}{2}\left(\frac{\partial v_i}{\partial x_j} + \frac{\partial v_j}{\partial x_i}\right) \qquad \textbf{(8)}$$

$$\rho\, {}^{D\boldsymbol{v}}\!/_{Dt} = -(\nabla\cdot \boldsymbol{T}) + \rho g \qquad \textbf{(9)}$$

$$ {}^{\partial\rho}\!/_{\partial t} + (\nabla\cdot \rho\boldsymbol{v}) = 0 \qquad \textbf{(10)}$$

The complexity of the mentioned constitutive equations has forced authors to focus most of the simulation works of flow behavior in two dimensions [33, 52, 57, 60-66]. This approach requires specific assumptions for specific situations leaving out the fact that granular materials in general could move easily from one layer to others making the profiles obtained from 2-D simulations different from those of the real behavior. Despite, these simulations in two dimensions describe moderately the average velocity in superficial layers.

In spite of the good agreement with that description, still as shear is applied to a real powder, dilation takes place and particles begin to move in the z-axis direction due to the new porosity in the bulk of the cavity causing three dimensional flow. Basically, there is an interchange of particle from the bottom of the chamber to the top and vice versa, giving the appearance that the surface has only convective movement in the top layer and not diffusive in the direction to the bottom. Therefore, there is the need of experimental results from simple devices clearly demonstrating the granular flow in the three directions so that the constitutive equations presented here can be validated.

1.2 Granular mixing

Granular mixing is a complex process determined by both the kinematics of the mean convective flow and local diffusive and segregation fluxes considering the random motions of particles and the differences in properties of the particles being mixed. Basic studies of powder mixing are needed to gain better understanding of the basic phenomena of powder flow and consequently for the improved design of industrial mixing processes. Up to now, regarding manufacturing in the industry, broad practical requirements are being satisfied with the industry worker experiences but design capabilities are still in general been sought. Solutions to mixing problems are sought by performing massive experimentation or by a smart sequence of statistically designed experiments.

Different approaches have been developed by researchers to obtain fundamental knowledge of granular flow to finally apply it onto mixing. One approach is mixture theory (or theory of interacting continua), which establishes that at any instant of time, every point in space is occupied by one particle from each constituent [52]. *Passman et al.*, (1986), [67] used this theory by applying concepts such as equilibrated forces and stresses, introducing an additional balance equation. Another approach is the averaging method, which consists in modifying point-wise equations of motion, valid for a single fluid or a single particle, to take into account the presence of the other components and the interactions between components. This approach describes the discontinuity conditions at moving boundaries between the phases [23, 52].

The cited methods require constitutive relations to make connections among kinematic, electromagnetic, mechanical, and thermal fields that are compatible with balance laws. In many cases those fields are ignored [55] to reduce the degree of complication of the generated equations. However, these fields have to be considered depending on the particle size in order to obtain an excellent description of the flow. For instance *Gudhe et al.*, (1994),

[68] employed thermal effects in their research considering the energy balance, finding that the parameter of viscosity and thermal conductivity vary with the volume fraction in a way that is consistent with the physics of the problem.

The common barrier of the above mentioned approaches to fully describe powder mixing is the large quantity of factors that govern powder flow such as density, wall-particle and particle-particle friction coefficient, restitution coefficient, angle of repose, angle of internal friction, electrostatic charges, surface properties, etc. The comparison of simulated results to real powder mixing loses meaning if careful control of factors is not imposed. Because of this degree of difficulty most prior studies have also considered only two dimensions [33, 52, 54, 61, 63, 69-71], hindering the real characterization of granular flows.

Another approach is to look at the individual particles using the technique discrete element method (DEM), which is a numerical model capable of describing the mechanical behavior of granular flow based only on force balances with simple models of inter-particle forces [72-79]. Unfortunately, the simulation of even a fraction of the real number of particles in commercial mixers requires a high computational power. Even with the advance in the technology nowadays, it is difficult to describe real situations of only a real few seconds and with a limited quantity of particle [77, 79]. Therefore the technique is somewhat impractical to develop a sound knowledge of the real behavior of powder flow or mixing [23]. On the other hand, experiments on devices designed to process targeted number of particles under known conditions along with the DEM technique could provide very useful information of the real behavior.

An additional approach is the use of sensors inside the mixers such as special cameras [8, 9, 18, 80] or NIR [81] to track the real behavior and sense the final point of mixing. However, real industrial applications require the understanding in three dimensions and only few studies in this line has been done, e.g. the use of new techniques such as positron emission particle tracking (PEPT), [82-84] and the use of MRI [61]. Unfortunately, at the present moment these two techniques are very expensive, complex, and difficult to have in a common laboratory [27] not mentioned in-line.

Other researchers have used a different alternative, the solidification or 'freezing' technique, which consists in pouring a binder over the mixed powder at the end of an experiment allowing its solidification inside the vessel [27, 85, 86]. The entire slab is cut into slices and each section digitally scanned and analyzed. The results obtained in three dimensions have shown that the effect of the additional axis in study cannot be neglected to make predictions.

An additional limiting factor to the complete understanding of granular mixing is the type of mixer used in the experiments. Most of the works to understand or monitoring mixing behavior have been focused on tumble blenders [87-91], which are the most used nowadays by the industries of solid handling. The progress has been substantial, however the complex geometry of mixers, which makes any analytical treatments more complicated has forced most of the work to be done in two dimensions [33, 52, 54, 61, 63, 69-71], what caused in turns that the fundamental understanding of the phenomena is still hidden.

A thorough understanding of phenomena such as consolidation, dilatancy, yield function, plastic theory, and mixture theory along with all the factors that govern the flow of granular materials and how these factors affect the granular concentration of different powders is critical to find the solution to the modeling of granular flow [23, 33, 35]. This knowledge would also allow the design of equipment to achieve the necessary level of quality of any granular product [26, 92-96].

Considering all the emblematic problems in granular behavior, this work focused on developing a simple system where the imposed rate of strain was varied following a periodic function which permits to study the granular material random movement and the mixing of granular material at different particle sizes and initial filling levels. The goal was to demonstrate experimentally the relevance of the importance of taking in to account a third dimension and to gain insights of the physical phenomena (compaction, dilation, interface slip, chaos) involved in the 3-dimension granular flow, using real powders with certain polydispersity on size. The system allows targeting specific phenomenon thus better understanding of it can be drawn from the experimental results to combine the experimental part with the mathematical analysis so that the results of these studies could also allow the phenomena be explained in a real basis. The development of models in this area of granular material is limited because most of the researchers have focused on mathematical simulations relegating the real behavior and experimental development to a second plane [48, 51, 97-99]. The results of these studies would allow to combine the experimental part with the mathematical analysis so that in the future the phenomena could be explained in a real basis.

1.3 Objectives

1.3.1 General Objective

To study the granular flow phenomena and its impact in the mixing process of a binary powder mixture in a device where the flow is induced by the stress applied by the movement of rough-surfaces moving walls

1.3.2 Specific Objectives

- To develop a simple system where the imposed rate of strain is varied following a periodic function.

- To demonstrate experimentally the relevance of the importance of taking into consideration the third dimension and to gain insights of the physical phenomena involved in the 3-dimension granular flow, using real powders with certain polydispersity on size.

- To study effect of wall amplitude, velocity, particle size, initial height in the Z-axis, in the mixing of the surface and in the Z-axis.

- To study the phenomena of granular material random movement, dilation and segregation in the system.

2 Experimental work

The experiments consisted in mixing two materials with similar properties, except the color, at different operating conditions in the mixing device that consisted of an open box with two moving walls and three static ones, as shown in Fig. 2. The wall motions were controlled by two step motors connected to a computer in a master-slave configuration. To study the mixing process, the particles with different colors (section 2.3) were loaded in to the chamber, mixed under different shear stresses, and the distribution of the particles tracked as a function of the time and space using image analysis (section 2.4).

2.1 Apparatus

The width (*W*) or space between the moving walls was fixed at 2.79 cm after previous experiments showed that this dimension together with a particle size of approximately 570 μm, produced enough transfer of momentum among the particles inside the chamber. This width and particle size represents a ratio of $W/d \cong 50$. The length (*L*) and height (*H*) of the chamber were 22.86 and 11.43 cm respectively which correspond to an aspect ratio *L/W* of 8.18. A schematic view of the equipment is shown in Fig. 2.

Coordinates were chosen as follows: plane x, y correspond to planes parallel to the surface of the cavity and plane y, z correspond to planes parallel to the vertical static walls, Fig. 7.

The entire device was made out of acrylic glass. The inside surface of the moving walls was modified to impart roughness so that enough friction between the walls and the particles was generated. This friction caused the particles closer to the surface to move once the walls started to move. The base and the static walls in the chamber were kept smooth.

In the base of the equipment two straight trenches were made with the width as equal as the width of the moving walls to direct the moving walls and avoid any entrance of particles to the trenches.

The length of the moving walls (71.12 cm) was large enough compared to the length of the chamber (22.86 cm) to run experiments at different amplitudes of the periodic function. The dimension of the base of the equipment was 64.77 cm in length and 24.90 cm in width to avoid any torsion or vibration of the moving walls during the experiments.

The top of the equipment is another acrylic glass flat slab with 1.9 cm of width, connected to the bottom of the equipment by four beams of 3.81 cm of diameter. This top flat surface had two straight trenches similar to the base where the moving walls fit exactly. These channels in the base and in the top surfaces together with the four beams that connect both surfaces were made with the aim of giving extra stability to the system. It was necessary in order to eliminate all kind of noise cause by any vibration because preliminary experiments show that particle distribution is highly sensitive to them.

The two moving walls were connected to two DC servo motors (model Baldor BSM80C-175AA) with two shafts. The software Workbench permitted to establish different speeds and amplitudes of the moving walls.

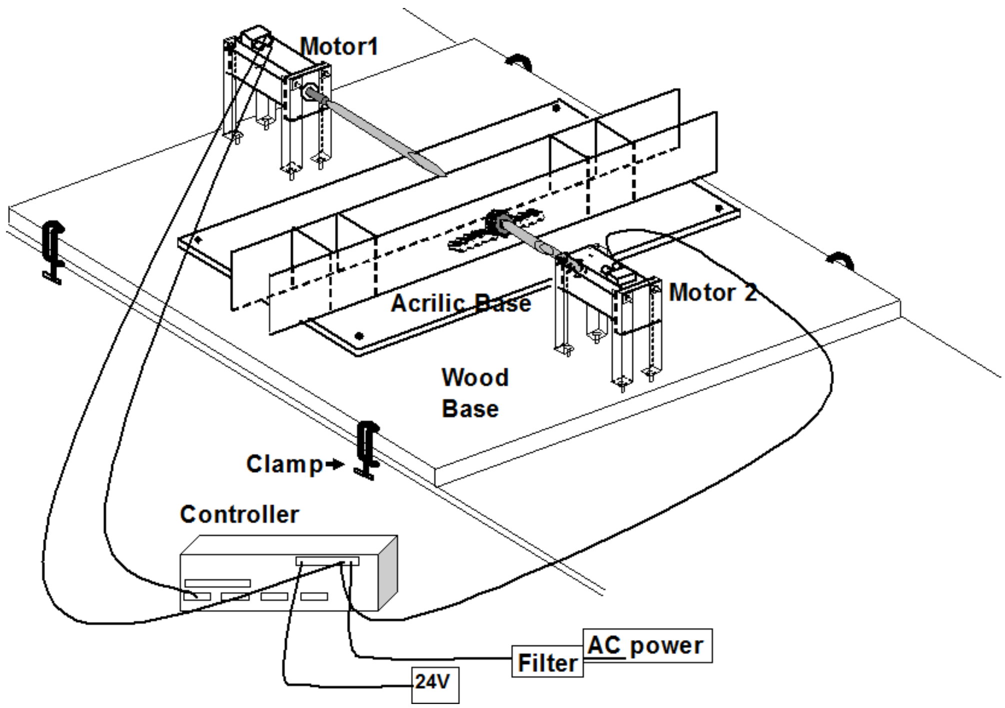

Fig. 2. Schematic of the oscillatory shear powder mixer

The function of the walls was as follow:

$$v = \begin{cases} a, cm/s \rightarrow if \;\; 0 \;\; \langle \;\; t, \sec \;\; \langle \;\; T/2 \\ -a, cm/s \rightarrow if \;\; T/2 \;\; \langle \;\; t, \sec \;\; \langle \;\; T \end{cases} \tag{11}$$

where T is the fundamental period, see Fig. 3.

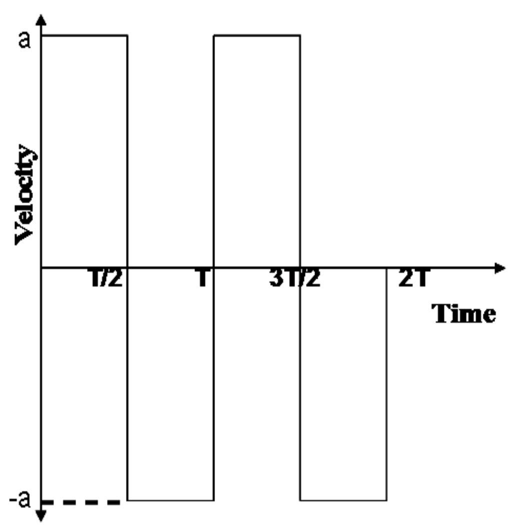

Fig. 3. Wall motions corresponding to periodic flow

Only a discontinuous flow was considered, (Fig. 3). The values of velocity were established to ensure sufficient transfer of momentum to produce movement of all the particles to achieve the desired mixing. However, it cannot be too high or it will produce problem in the control system at the moment of making the sudden stop of the wall to change direction.

2.2 Computer control system

The motors were connected to two integrated motion controllers (FlexDriveII FPH1A02TB-RN23 115 VAC) for rotary and linear positioning. The controllers were connected to a computer with the software Workbench to control the motors. One control functioned as the master while the other as the slave.

2.3 Particle formation

The experiments were performed with granular material prepared from lactose with and without color. The preparation of the white and blue particles followed the summarized procedure:

- **White particles**

Lactose Monohydrate with a particle distribution in the range between 60 to 250 µm was poured into a cylindrical high shear mixer with a capacity of 460 g. The mixer was started at 560 rpm for 30 seconds, after which water was sprayed onto the lactose following the procedure used by Realpe (2006), [100]. The granulation was made at different levels of humidity to obtain the higher quantity of particles of the desired sizes of study (600-425µm), (710-600µm), (850-710µm) and (1400-1000µm). After each granulation the particles were scattered in a large surface to dry at ambient temperature for one day. After the dried step, powders maintained a low humidity of approximately 0.5% (w/w). The powders were non hygroscopic. The dried powders were then sieved for 30 min. The sieves used for particle-size classification were Tyler's 40, 30, 25, 20, 18 and 14 US Standard testing sieve 8 inches in diameter. The Mesh Sizes are shown in Table 1. The sieving was made using Tyler's RX-24 sieve shaker.

Table 1. Corresponding Nominal Sieve Opening of the used sieves

Standard US	Standard ISO	Standard US	Standard ISO
No.14	1400 μm	No.25	710 μm
No.18	1000 μm	No.30	600 μm
No.20	850 μm	No.40	425 μm

Subsequent to sieving, all the samples inside each mesh were submitted to a vacuum system in order to eliminate extra fine particles adhered to the surface of big particles. It was necessary in order to avoid cohesivity and effect of electrostatic charge in the movement of the coarse particles.

- **Blue particles**

The same Lactose Monohydrate was used to create blue particles. An organic blue ink powder was used to vary the white color. The ink powder had a density of about 0.2 g/cm^3. The blue powder was added to the lactose in order to prepare mixtures of 97.5% (w/w) of lactose. Because of the high percentage of lactose and the low density of the ink powder, the blue particles created had similar density as the white particles of the same size, Fig. 5, showing a difference in density of about 0.03 g/cm3 which is so low to produce segregation by density when mixing [8]. After that the same granulation process mentioned for white particles was implemented. The drying process was different because the wet granules were introduced into an oven at 95^{o}C for 30 min. The temperature and time were chosen after a previous experimental design. This process made sure the blue particles get impregnated firmly in the surface of the white particles. The same process of sieving and vacuuming applied to the white particles was applied to the blue particles.

Pena *et al*., 2007, [114] and Cleary, 2008, [113], have demonstrated that the shape of the particles is a strong factor in the variation of particle distribution, consequently this factor was blocked in this study. **Error! Reference source not found.** shows a sample of the shape of the particles. They have a regular shape similar for all the sizes. Blue and white particles of each size have a similar surface, thus causing no effect in the results obtained of particle distribution. This particle shapes were neither acicular nor flat as can be seen in **Error! Reference source not found.**, however there is a lot of roughness in the surface supplying enough friction to produce a good transfer of momentum among particles. These powders exhibited no cohesiveness and thus flowed easily presenting and angle of repose of approximately 25^o.

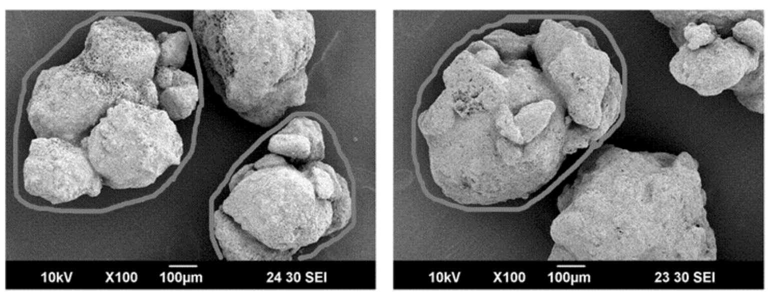

Fig. 4. Shape of the particles a) blue particles b) white particles

Once the preparation of the blue and white particles was finished, it was proceeded to measure their particle distribution in the ranges of study by image analysis. Fig. 6 depicts the equipment used to obtain and process the images to obtain the particle distributions. Table 2 describes the various parts of the vision system and the software.

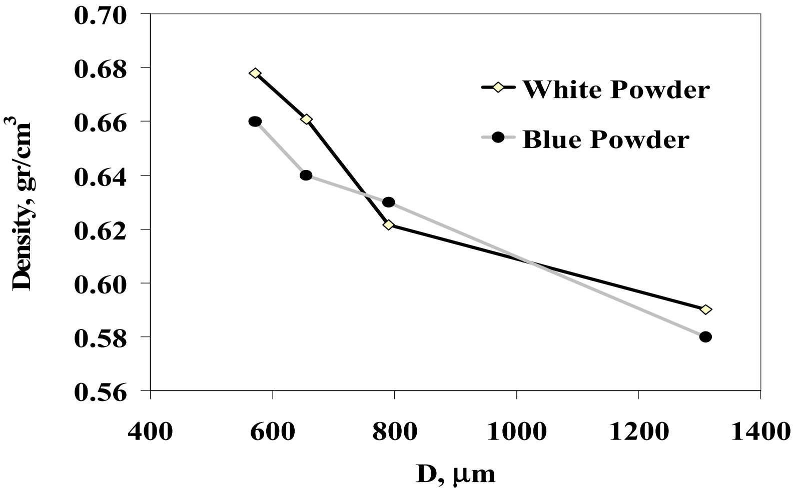

Fig. 5. Difference in density between the blue and the white powders in the range of particle size studied

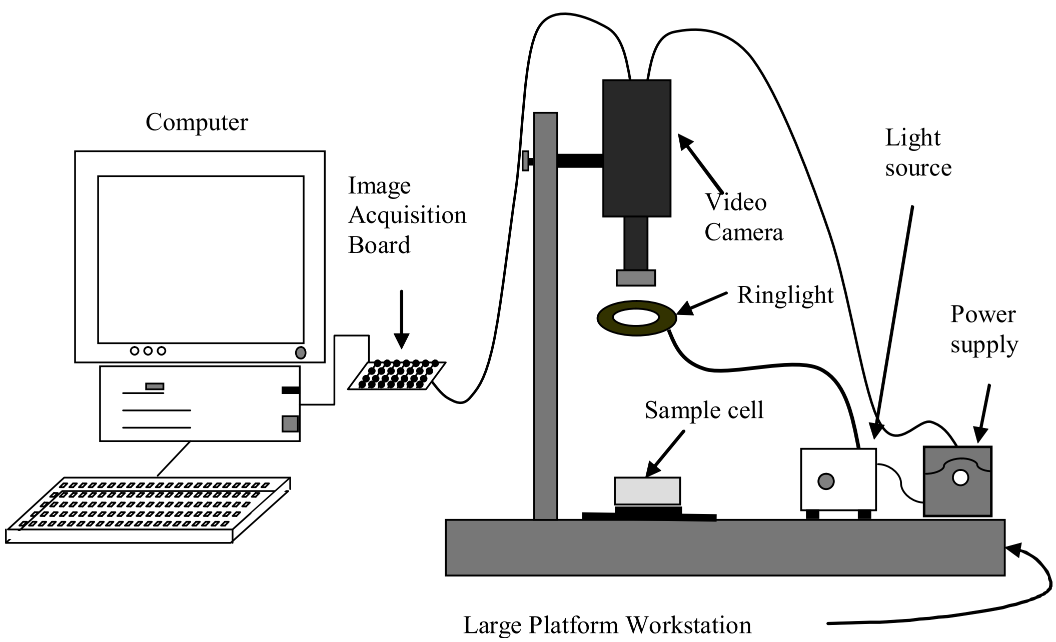

Fig. 6. Vision system schematic

Table 2. Equipment and software used to acquire and analyze images

Equipments and Software	**Description**
Color Image Acquisition Board	Model: IMAQ PCI-1411 (National Instrument)
Color CCD Camera	Model: GP-KR 222 (Panasonic)
Illumination System	Model: STOCKER&YALE fiber optic illuminator model 20 (quartz halogen lamp)
CCD Lens	Model: 10X CCD C-mount lens (Close focus zoom lenses, Edmund Industrial Optics)
Base Software	Matlab, Microsoft Excel
Image Processing Software	IMAQ Vision 6.0 for LabView 6i (National Instrument)
Statistical and Technical Graphing Software	SigmaPlot 2000, Minitab 15

The images obtained by the color CCD camera were digitized by an image acquisition board to yield images 640×480 pixels in size. All the images were taken using the illumination system that stabilizes the intensity of the light.

2.4 Mixing patterns visualization

The main chamber of the oscillatory shear powder mixer was divided in two by placing a divisor exactly at the center, parallel to the moving walls and with the same length of the chamber (22.86 cm). In one side it was poured the blue particles, and the white particles in the other side. Then, the divisor of the chamber was withdrawn to have the powders arranged parallel to the moving walls.

A digital camera with high resolution and fast shutter speed to freeze images at high velocities was installed at the top of the equipment perpendicular to the flow field. The working distance was 45.72 cm from the lens to the surface of the material. As movement was applied to the walls and the powders began to mix gradually with time, the camera was used to take periodic shots to study the distribution of the particles at the top surface as function of time.

To study the movement in the three dimensions, a solidifier was poured slowly over the mixed powder at the end of the experiment. Before pouring the solidifier, four very thin plaques (0.05 cm) were introduced between the walls and the powders to protect the walls which are soluble in the solidifier. The plaques did not cause any effect in the final distribution of the particles. The "wetted" sample was then dried for 10 min, after which it was withdrawn from the equipment and placed in a hood for a whole day until completely dried. Finally the entire slab was cut vertically in 8 slices each with the same length Fig. 7. Pictures of each slice were taken to study the distribution of particles in the vertical layers (y and z axes).

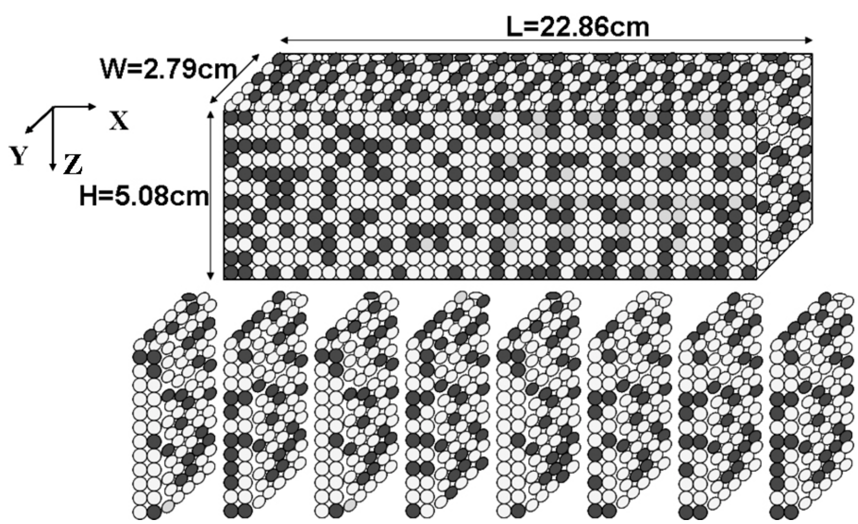

Fig. 7. Scheme of the samples taken with the real dimensions. Main sample cut into several slices.

3 Mixing of Granular Materials: Effect of Periodic Shear

In this chapter, the oscillatory shear powder mixer was used at different wall velocities and wall displacements. The goal was to obtain a deeper understanding of the internal behavior of granular material in the three dimensions as a function of the manipulated factors. The results reveal that the best mixing was found near the moving walls and in the superficial layer. A triangular pattern was obtained at the bottom of the mixing chamber whose size depended on the length of the mixing chamber and the velocity and wall displacement. The phenomena of dilation, consolidation and segregation played an important role in the mixing performance.

3.1 Introduction

The study of granular material behavior is gaining more relevance in recent years because of the need to have higher quality and reliable products. The length of mixing in the majority of the occasions in most of the industries is established by trial and error and depends on results of laboratory analysis of samples taken as well as the experience of the worker in charge of the process [81]. Nowadays, these industries are focusing on decreasing the time of production while maintaining a high quality manufacturing, requiring thus more knowledge about stopping the process at the exact time of reaching the best mixing.

The general purpose of most of the study about granular materials has been basically to understand the basic real behavior of the powders inside the mixers. Many factors have been studied in these mixers such as degree of inclination, velocity of rotation, blade velocities, blades shapes, filling height, vibration, etc., but the most used is the velocity of rotation because of its high effect in the mixing caused by the transfer of momentum that walls give to the particles. This effect of velocity together with other factor gives valuable information about mixing behavior inside a mixer, however there is still a great deal of details that are hidden because of the complexity of designing three dimensional experiments where real phenomenon about granular behavior can be obtained. Therefore, there is a need for simple idealized flow experiments that nevertheless capture the basic physics found in 3 dimensions in powder mixers.

This chapter presents the results obtained in the oscillatory shear powder mixer as the two powders were mixed manipulating the wall velocity and amplitude. The results presented suggest that velocity is the most important parameters although amplitude plays a role as important as velocity.

3.2 Experimental conditions

Two operating conditions were considered in this study: wall amplitude and velocity. Three levels were used for the amplitude, (11.43 cm, 22.86 cm, and 34.29 cm) and three for the velocity (9 cm/s, 13 cm/s, and 16 cm/s). A scheme of the factorial experimental design is shown in Fig. 8. The number 2 in each circle refers to the number of replicates. The speed of the walls was confirmed with a tachometer. The error of displacement measured was about ± 1mm. The walls moved always in opposite direction.

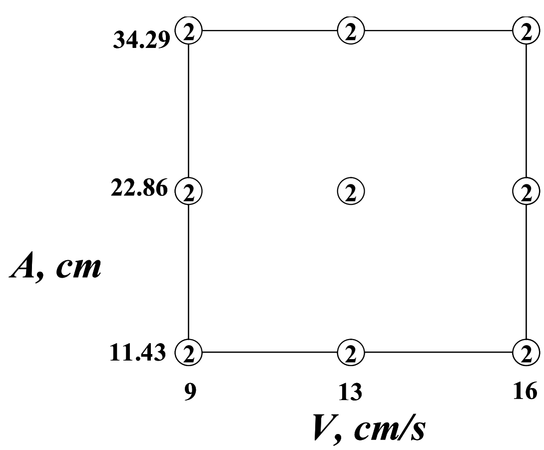

Fig. 8. Two-factor factorial experimental design with three levels, central point and 2 replicates

The particle size distribution (PSD) used was in the range of 425 – 600 μm. Table 3 includes the statistics of the particle size of both powders (blue and white).

Table 3. Particle size distribution (425 – 600 μm)

Descriptive Statistics	Blue particles	White particles
Mean, μm	566.5	571.7
Median, μm	550.5	573.4
Standard Deviation	94.5	103.7
Kurtosis	1.3	1.0
Skewness	0.5	-0.3
Confidence Level	3.3	4.4

The distribution of particles was narrow enough as to avoid the phenomenon of segregation by particle size.

These powders exhibited no cohesiveness and thus flowed easily. The flow factor by Jenike (ff) [101] were: dark powder, ff ≅ 26 and white powder, ff ≅ 25. This flowability characteristic makes these powders to move quickly changing direction easily facilitating the mixing.

3.3 Results and Discussion

3.3.1 Effect of amplitude and velocity of the walls on mixing of unrestricted powder at the top surface of the cavity

Fig. 9 illustrates an example of the top view of the experiments at different experimental conditions showing the granular movement as a function of time (number of cycles), the shear rate imposed, and the amplitude or distance traveled by the walls. This figure shows that an increase in the shear rate, maintaining the amplitude constant, caused the mixing to increase. In the other hand, the mixing increased as the amplitude increased while maintaining a constant shear rate. However, velocity had a larger increase in mixing degree.

It is important to emphasize that these surfaces were open to the air thus it experienced zero friction and normal stress. At the beginning of the experiments the powders presented a specific volume and as shear stress was applied, the volume increased or dilated due to the free normal stress. The volume kept expanding until it reached the equilibrium point of changing volume where the bulk density did not change anymore. In other words the powder reached the critical state point on a given yield locus where the powder deformed without any change in its volume [23].

In summary, the larger the velocity (shear rate) and the amplitude, the faster the materials were mixed. This is due to the larger the velocity the larger the dilation or void fraction thus the easier the particles could move randomly between other particles. Similarly, the larger the amplitude the larger the time the material is exposed to the large dilation and thus the faster the mixing. Moreover, the time showed by the different experimental conditions could be related to the time the same powders would take to mix in the open-to-the-air zones of industrial mixers.

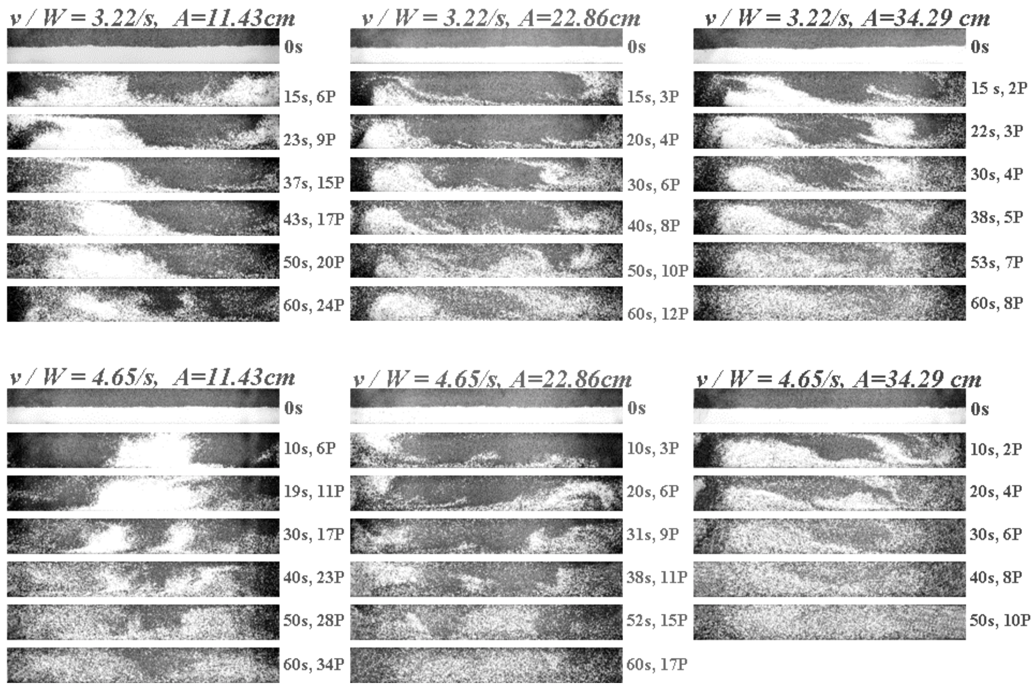

Fig. 9. Variation of mixing in the superficial layer (x,y axis).
Effect of velocity and amplitude, 425-600 μm

As can also be seen, at the beginning of the experiment the material tended to group in some areas of the chamber. This is not an effect of static electricity since the average diameter is way higher than 30 μm [102] but rather the effect of shear rate. For the first cycle, the shear rate moved the material in the same direction of the wall movement however no mixing occurred since the material did not have enough time. After several cycles, the time was enough to permit the particles to move between their neighbor particles increasing the mixing. However, as can be seen too, for small velocities and amplitudes (left top corner in Fig. **9**), the particles tended to keep moving as a rigid solid making the mixing inefficient. This is due to the small dilation and the high recurrence of relaxation events.

The mixing dynamics of the surface was further quantified by the relative standard deviation (*RSD*). This particle concentration was calculated using a method similar to the one employed by Arratia et al., 2006, [17], but using instead the superficial domain. The picture of the entire *xy* surface was divided into "*n*" sectors. The particle concentration was then determined by counting the number of particles of each color inside each sector [8, 9]. Mixing rates were then constructed by plotting the relative standard deviation (*RSD*) as a function of time (Number of cycles) and operating conditions Fig. 10. The relative standard deviation was computed as:

$$RSD = \frac{S}{\overline{C}} \tag{12}$$

where

$$S = \sqrt{\frac{\sum_{i=1}^{n}(C_i - \overline{C})^2}{n}} \tag{13}$$

S, is the standard deviation, n is the total number of samples in the superficial layer, $\overline{C}$ is the average concentration in the entire layer, and C_i is the concentration in the *i* sector.

Values of *RSD* higher than 1 in Fig. 10 are the result of an increase in the volume of the blue powder giving a result of higher percentage of blue color in the surface at the beginning of the experiments. In addition, it can be seen that the *RSD* decays exponentially with time [21]. The *RSD* curves were fitted to the expression, $RSD = RSDmax - (1 - e^{-\theta P})$ with values of θ of 0.088, 0.250 and 0.282 (white circle, triangle and black circle respectively). The exponent θ is the average Lyapunov exponent and, since it is positive, it says that the time-periodic flow was in general chaotic [103]. Therefore, the systems evolve with time exhibiting a dynamic that manifests itself as an exponential growth of perturbations in the initial conditions, making the system to appear to be random. The higher the Lyanpunov, the more chaotic the dynamics and the faster the mixing.

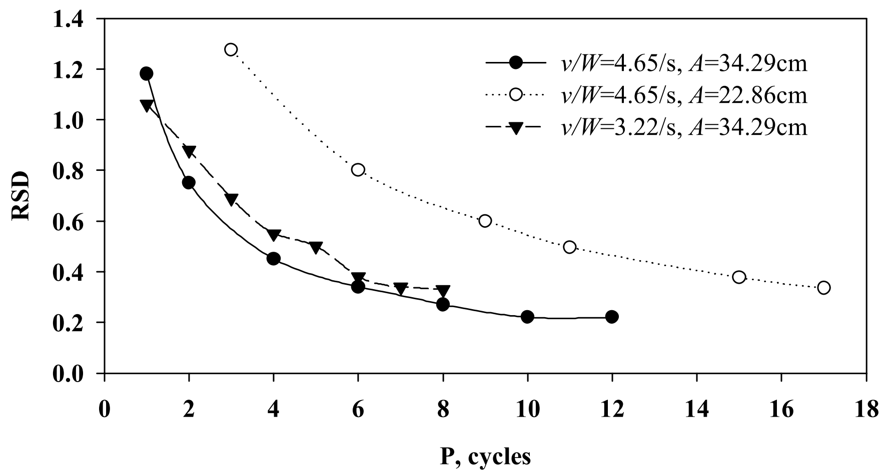

Fig. 10. Mixing rates in the surface as function of time, amplitude and strain rate imposed.

Focusing on both ends of the chamber, it can be seen that the mixing degree is higher at any moment until complete mixing is achieved. At the ends, the particles that were coming in the same direction of the moving wall collided with the static wall making the particles to change direction orthogonal to the direction of the moving wall. Since the amplitude of movement of the wall was larger than the length of the static walls, particles traveled the distance of this static wall and then changed their direction again but moving now in the same direction of the other wall which is moving in the direction contrary to that of its parallel wall. This change in direction combined with the collisional diffusion of particles due to dilation made the mixing in this zone higher than in any other part of the chamber. This behavior suggests that intermediate baffles along the chamber or for that matter, in tumble [21] will decrease the mixing time.

The application of shear to the walls in the x axis creates convective motion of the particles next to the walls. However these particles do not move along streamlines [104] as liquids do but rather in a totally random motion in the y and z axes. This is due to the dilation of the powders [60, 105] which causes the diffusion flux to be anisotropic [106]. Because of this random phenomenon exact replicas of each experiment could not be obtained, however since convective movement dominates the diffusive one, similar behavior was rather obtained.

3.3.2 Effect of amplitude and velocity of the walls in the z-axis (height) of the cavity

Fig. 11 shows the behavior of the distribution of the particles in the z direction after 60 seconds of applying shear. There are 8 vertical slabs showing the z-profile as a function of the x position in the chamber. Each slab depicts similar overall distribution although there are small differences. At the top of the slab, it was obtained the higher mixing when compared to the material closer to the bottom. The top surface (open to the air) experienced the lowest friction and highest dilation. On the contrary, at the bottom wall which is static, the particles received all the weight of the particles above and therefore experienced the highest friction. The material next to the moving walls exhibited a high mixing too due to the maximum velocity (maximum dilation) obtained at that region as a consequence of the shear and normal stress given directly by the walls. This high velocity facilitated the transport of particles in the z axis.

The high friction at the bottom wall caused a dissipation of the shear stress exerted by the moving walls. The lack of shear rate in that region caused a triangular profile (see Fig. 11a and Fig. 11b) that had the maximum height at the center of the chamber and decreased toward both ends. The height decreased toward the ends of the chamber due to the high mixing in this region, caused by the change in direction, as discussed above. The effect of change in direction disappeared toward the center of the chamber, thus the triangle height increased toward the center. Similar behavior was obtained for other experiments but the size of the triangle changed depending on the values of amplitude and velocity of the walls, Fig. 12.

(a)

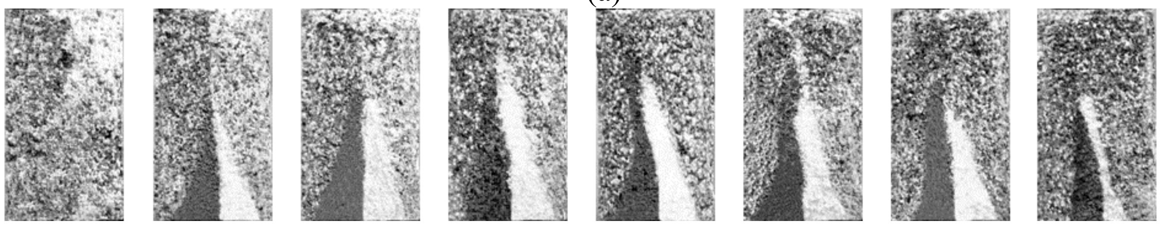

(b)

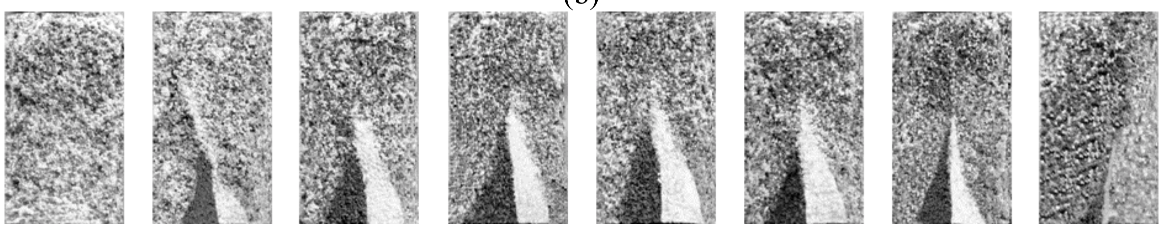

Fig. 11. Distribution of particles in the vertical layer at t=60s. a) v/W=4.65/s, Amplitude= 22.86 cm. b) v/W=4.65/s, Amplitude= 34.29 cm.

Comparing Fig. 11a to Fig. 11b, it can be seen that the triangular shape (specially the height) decreased as the amplitude was increased meaning that the overall mixing obtained in each slab increased. For large amplitudes, particles remained dilated for longer period of times making the process of collisional diffusion to affect longer near walls enhancing the mixing. This effect decreased near the bottom because of the zero velocity in this zone. Fig. 12 depicts the triangle height as function of the shear rate imposed and moving wall amplitudes.

The formation of the triangle due to the zero velocity near the static wall suggests that mixers with static outer walls will be less efficient than those that impart any kind of movement to the outer shell.

(a)

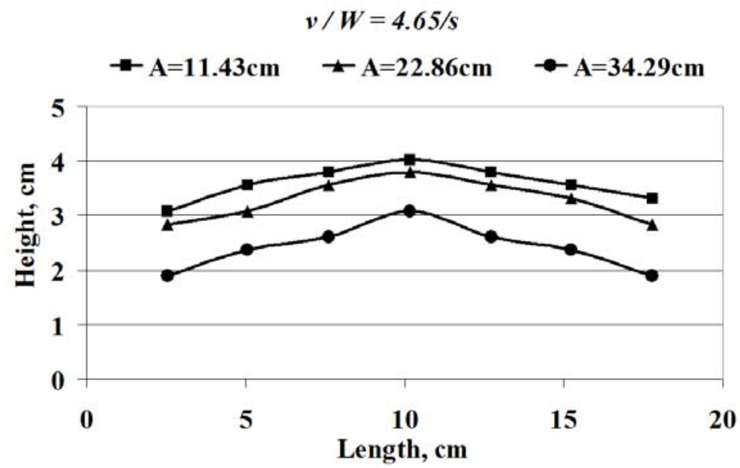

(b)

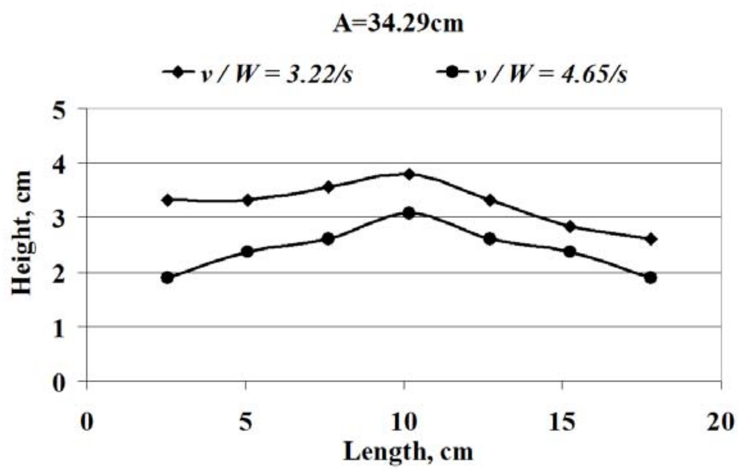

Fig. 12. Tendency of the maximum height of the triangular behavior along the x axis a) maintaining constant strain rate imposed and b) maintaining constant amplitude.

Plotting the tendency of the triangle height of the center of the cavity against the wall amplitude (Fig. 13), it can be seen that the triangle height decreases asymptotically tending to a constant value in the three curves presented. This could be so since an increase of the amplitude only maintain the dilation of particles for more time causing that the system to get the random mixing faster.

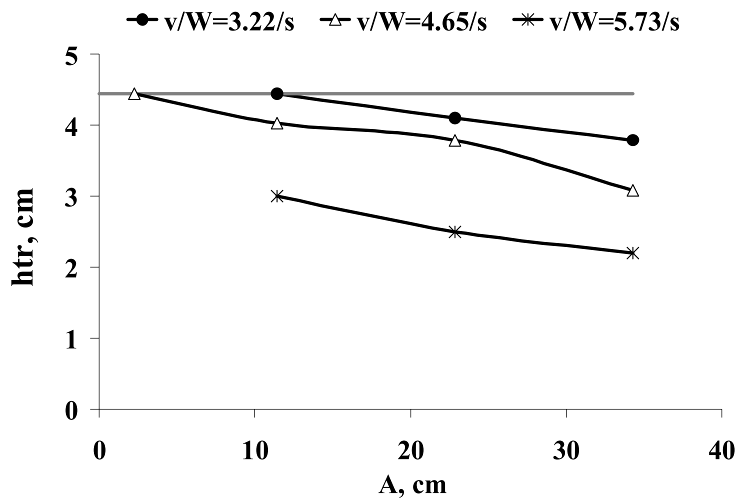

Fig. 13. Tendency of the height of the triangle in the center of the cavity as wall amplitude is increased at different wall velocities

Fig. 14 depicts the large decrease in triangle height with increase in the imposed strain rate. The tendency shows that the triangle will disappear if the velocity is increased infinitely making that the transfer of momentum in the bottom surpasses the friction wall-particle eliminating completely the static zone.

Considering the tendencies shown in Fig. 13 and Fig. 14 it was found the following correlation, with a high coefficient of determination or R-squared value.

$$\begin{aligned} htr &= 1.9107 + 0.3499V - 0.0228V^2 + 2.1092e^{(-0.0403A)} \\ R^2 &= 0.977 \end{aligned} \tag{14}$$

The above correlation follows clearly the tendency of the parabolic behavior of the *htr* with the velocity and the exponential decrease with the amplitude to a constant value. The extrapolation values of amplitudes and velocities give logical values of *htr*, however this has to be demonstrated experimentally.

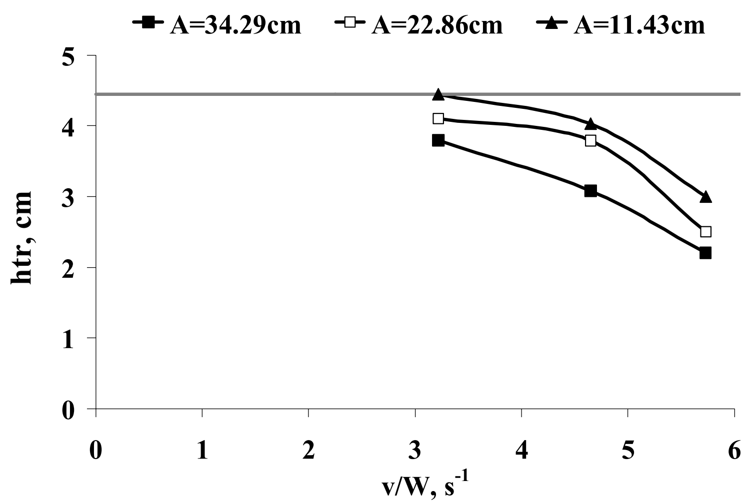

Fig. 14. Effect of the imposed shear strain rate on the height of the triangle in the center of the cavity at different wall amplitudes

An additional experiment was performed to corroborate the particle movement in the z axis. The experiment consisted in ordering the two materials in a two layers fashion, one above another, and mixing the powders using the same operating conditions. Fig. 15 shows the beginning of the experiment (a) and the final state (b). It is evident the movement in the z axis indicating that this axis has to be considered when trying to simulate powder flow. As it is shown, white particles located at the top (a) moved downward penetrating the blue powder in the extremes, specifically near the moving walls, creating the mixed material and the no-mixing triangle again. Furthermore, there was movement of the blue particles toward the top, which confirms that the dilation was higher toward the top and thus blue particles were easier to be pushed upward by the force exerted by the downward movement of the particles near the moving walls. The same behavior was obtained when the materials were inverted in position.

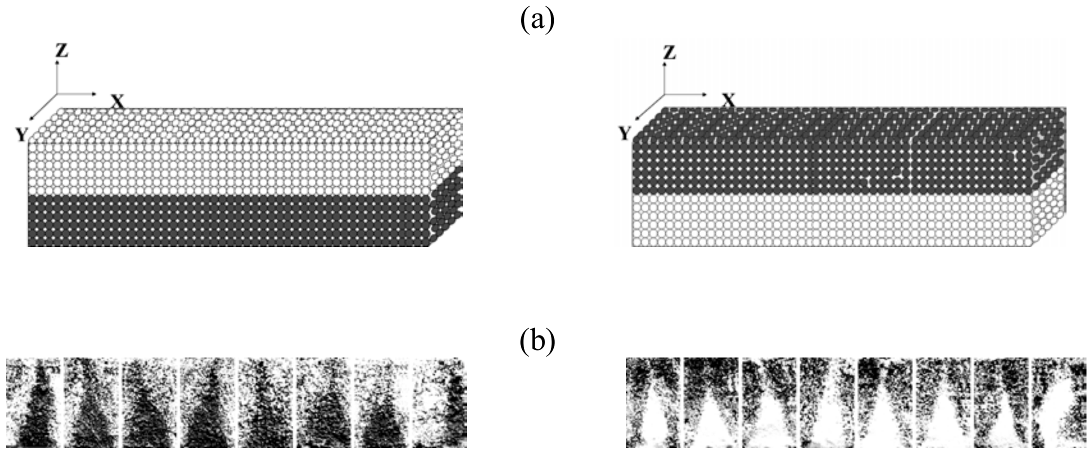

Fig. 15. Behavior in the z axis (a) Initial arrangement at t=0 sec.
(b) Final distribution at t= 60 sec.

The degree of mixing in the z axis was again quantified by the relative standard deviation based on the concentration of particle by sectors along the x axis from one extreme to the other of the chamber for all velocities and amplitudes.

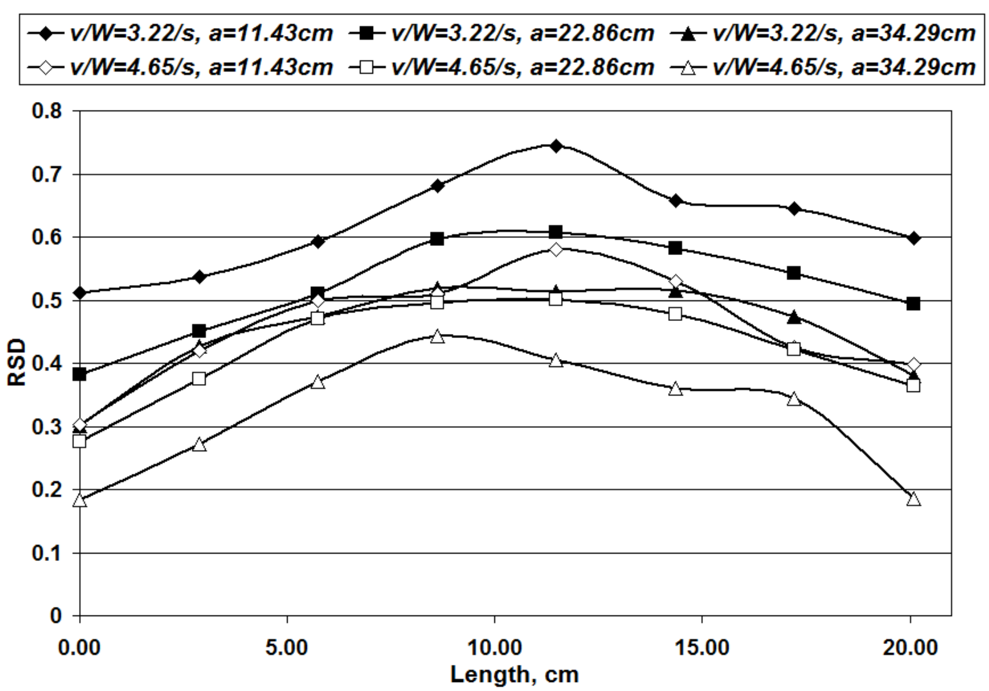

Fig. 16. Effect of the shear rate imposed by the walls and the amplitude in the mixing profile of the vertical layers

Further analysis shows that a small increase in velocity by a factor of 1.3 caused a decrease in *RSD* of 33% which is similar to the decrease caused by an increase in amplitude by a factor of three. Therefore, velocity is important for the dilation and the amplitude to sustain it.

3.3.3 Behavior of segregation on the surface and in the z-axis of the cavity

Additional experiments were performed to study the segregation in this system caused by difference in particle size. Fig. 17 shows the behavior in the vertical layers of small white particles 425-355 µm being mixed with big blue particles 710-600 µm. The triangle profile obtained in the mixing experiments of particles of similar sizes (no segregation) appears here too in the mixing of particles with different sizes. However, the distribution is rather different. It can be observed that the blue particles tend to move up to the surface more easily than the white particles. The small quantity of blue particles compared to white one in the triangle confirms this tendency. Considering the dilation in the system, the total porosity will increase when shearing is applied making small particles percolate through void fractions from the layer in the surface to layers below resulting in a net segregating flow of the smaller particles in the downward direction.

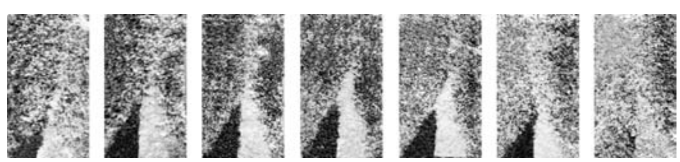

Fig. 17. Distribution of particles in the vertical layer at t=60s, *v/W*=4.65/s, Amplitude= 34.29 cm, Blue 710-600 µm, White 425-355 µm

Fig. 18 shows the results for a similar experiment (same operational conditions) but interchanging the sizes, now the white where 710-600 µm and the blue 425-355 µm. The distribution of the particles in the *z*-axis is completely different indicating that the small differences of particle properties of the powders blue and white increases with the size. Again the big particles (white in this case) tend to move faster to the surface but in a different way. This behavior can be observed in the surface of the cavity in the pictures presented in Fig. 19 where the relation of white to blue particles in the surface increases with the time due to the segregation by size being an evidence of the particle distribution in the vertical layer, *z*-axis.

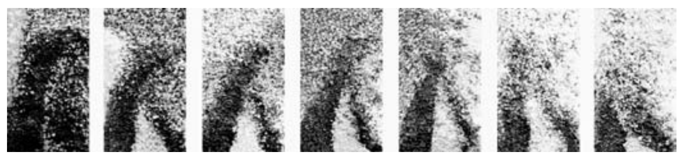

Fig. 18. Distribution of particles in the vertical layer at t=60s, *v/W*=4.65/s, Amplitude= 34.29 cm, White 710-600 µm, Blue 425-355 µm

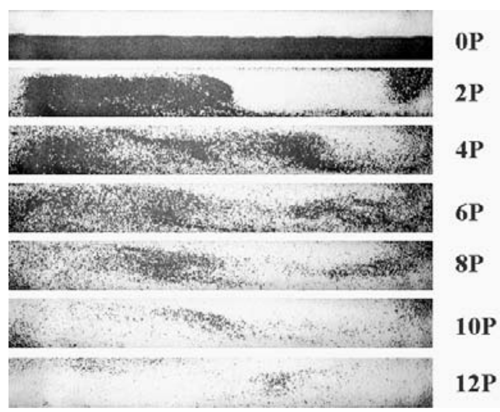

Fig. 19. Distribution of particles on the surface layer at t=60s, *v/W*=4.65/s, Amplitude= 34.29 cm, White 710-600 µm, Blue 425-355 µm

The *RSD* in the surface was plotted versus the period in Fig. 20. The continuity in decrease of the curve below the dashed line or random mixing line is an indication of segregation in the system. The longest the separation, the highest the segregation.

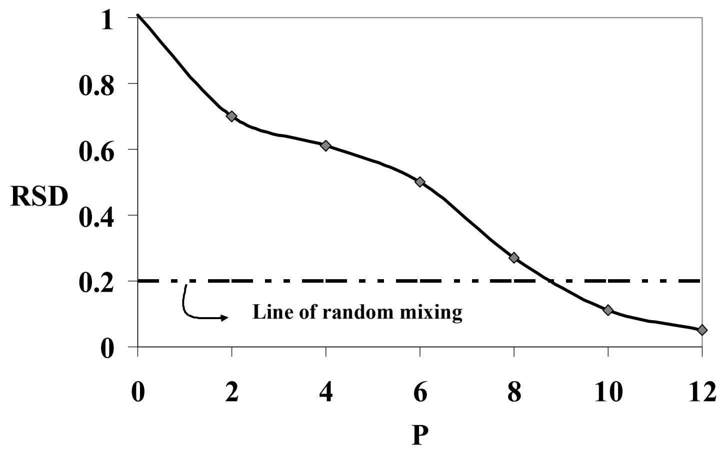

Fig. 20. Effect of segregation. t=60s, *v/W*=4.65/s, wall amplitude= 34.29 cm, White 710-600 µm, Blue 425-355 µm

Therefore, additional studies of the behavior of segregation in this system are necessary to relate the segregation to differences in particle properties when mixing. Plots such as Fig. 20 serve as detectors of problems in the mixing due to segregation or due to problems in the velocity of the walls.

3.3.4 Effect of time and wall perturbation in the z-axis of the cavity

As it was mentioned in section 2.1, the particle behavior is highly sensitive to any perturbation or noise in the wall movement. Some experiments to verify and quantify this phenomenon were done changing the velocity of one of the walls with a small perturbation as shown in Fig. 21. The total velocity of both moving walls was the same, 9cm/s, but a sudden stop was applied to one of them to create perturbation. The white particles were in touch with the perturbed wall during all the set of these experiments.

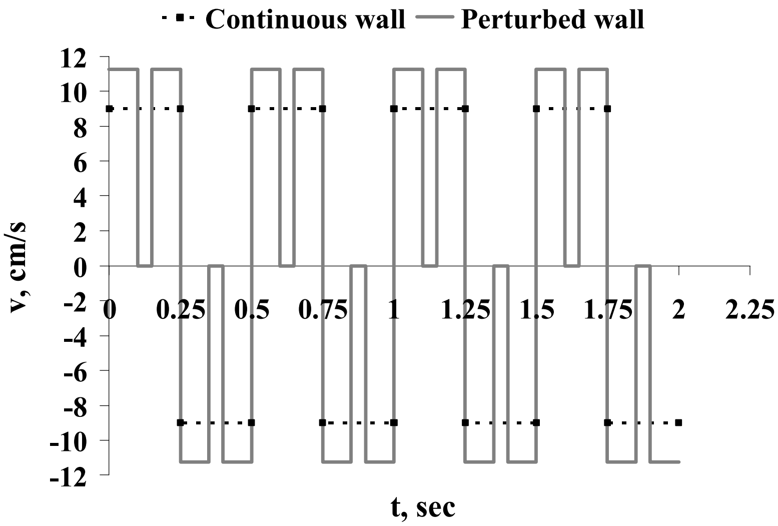

Fig. 21. Wall motions corresponding to periodic flow

As can be seen in Fig. 22, there is a large difference between the behavior of the experiments of continuous (CW) wall and perturbed wall (PW). At 60 seconds of mixing there is no visually difference bettering the degree of mixing, however at 140 sec it is noticeable that the perturbed walls produced a higher mixing.

The perturbed wall generates changes in dilation in the zone near them. The dilation in this zone (region of white particles) increases suddenly with the perturbation and in a higher quantity than in its contrary zone (region of blue particles) and decreases in the same way when perturbation finishes. These changes creates sudden increases in the porosity as well in the zone of white particles making that blue particles penetrates this zone softly creating a parabolic profile as seen in Fig. 22. As the time goes on, the parabolic profile is more pronounced as depicted in Fig. 23 due to the effect of porosity, however the same effect makes the blue particles distribute faster as it penetrates the perturbed zone together with the white particles.

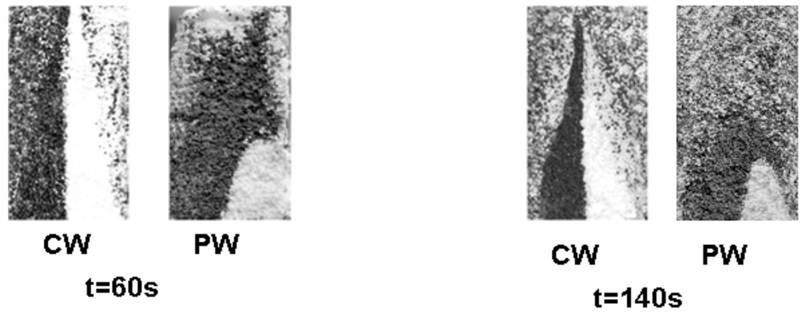

Fig. 22. Difference in particle behavior in the *z-y* plane between experiments with continuous moving walls and perturbed moving walls

When time increases the profile in the z-axis shown in Fig. 23 will remain constant as in t=140s. The static zone will stay as shown and the motion zone will get its random mixing.

The quantification of the mixing for each picture in Fig. 23 is shown in Fig. 24 by plotting the *RSD* versus time.

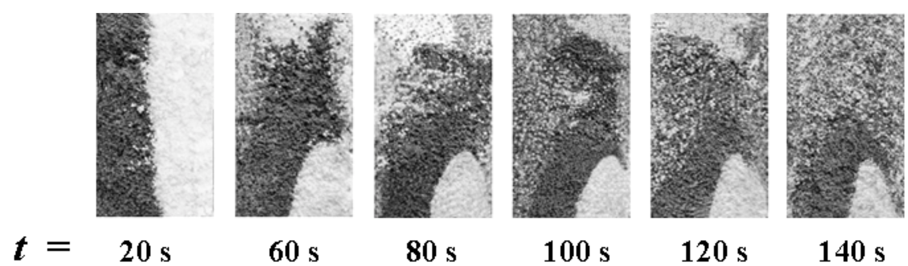

Fig. 23. Effect of time in the z-axis of the experiment with perturbed wall

It is shown clearly that the mixture will not reach its complete random mixing (*RSDr*=0.2) increasing the time due to the effect of the static wall in the bottom. However, the motion zone (zone above the parabolic profile) will reach the random mixing making the curve to obtain stability at approximately *RSD*=0.5. This is the maximum mixing it can be obtained when applying perturbation to one of the walls. On the other hand, the experiment with continuous wall movement will produce the other curve in Fig. 24 (line with squares), which levels out at a higher value of *RSD*, approx. 0.69. The difference of the zone of stability is observed in Fig. 22 at 140 seconds and it is due to the size of the static zone which is noticeably higher for the experiment with continuous wall velocities.

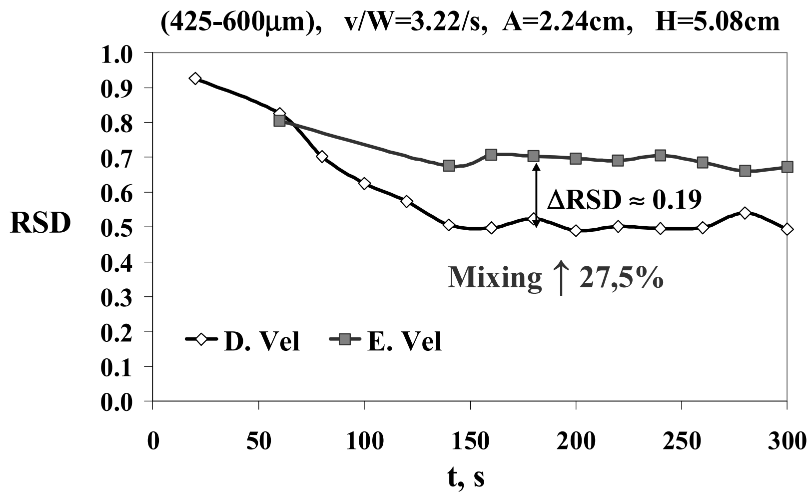

Fig. 24. Mixing rates in the surface as function of time for the system with equal velocity in the walls (E. Vel) and different velocity in the walls (D. Vel)

It can be observed that even a small induced perturbation to any of the walls will cause a markedly effect in the dilation of the powders in the cavity and thus in the entire mixing with an improvement of 27.5%. This result suggests that similar patterns could be used to increase mixing in industrial mixers and thus lower times.

3.4 Conclusions

The device developed in this study was able to mix two materials of similar properties under adequate operating conditions. It was demonstrated that mixing of granular material requires a minimum force (minimum velocity) to cause sufficient dilation and maintenance of the dilation. It was confirmed that the use of baffles helps in increasing the mixing performance in mixer such as tumble and screw or ribbon ones. The static wall at the bottom decreased the mixing performance by dissipating the shear rate through friction. Granular material move randomly once sufficient dilation is generated thus simulation works must consider the three dimensions. In a mixer with continuum movement of the walls or paddles, velocity is the key parameter for the mixing performance.

A triangle with no mixing was found in the z axis whose characteristics depended on the changes in amplitude and velocity of the walls. Limitation of area of contact between particles and static walls and high speed of moving parts increase the mixing performance.

The shape of the triangle is altered with the presence of segregation. It can be identified easily if the mixing never reaches its random relative standard deviation which can be by detected following the curve *RSD* vs. time.

It can be noticed that any perturbation in the system varies the total mixing in the cavity. Perturbation or noise by vibration increases the dilation enhancing the movement of particles in all direction increasing the total mixing in the cavity as well.

The device could be used to characterize the mixing performance of powders with different properties in different type of mixers. Therefore, additional experiment with different material must be performed.

4 Effect of Particle Size in Mixing of Granular Materials Under Periodic shear

In this chapter experiments in the oscillatory shear powder mixer were run at different particle size distributions and wall displacements. Results expose that the faster mixing is obtained for particles of larger diameters. Mixing in the superficial layer follows a chaotic trend whilst a triangular pattern was obtained at the bottom of the mixing chamber whose size depended on the wall displacement and the particle diameter. The phenomenon of dilation was remarkable, varying the expansion of the bed linearly with the particle size.

4.1 Introduction

Different experimental conditions have been studied in many blenders such as shear stress applied, dimensions of the blenders, filling height, etc., obtaining important results in particle flow and mixing, however, the rheology of granular materials is still of concern in these applications. The reasons lay in the amount of particle properties that can affect the distribution of particles hindering the real characterization of granular flows.

One of the most important factors in the study of granular flow and mixing is the effect of particle size. The majority of the work done about this issue has focused in segregation [17, 89, 106-111] and few works have focused on the effect of changing the entire particle size in a system to study the distribution of particles. The latter works were performed in two dimensions with monosized particles [33, 54, 60, 62, 65, 69-71, 112]. Furthermore, until now none of the proposed constitutive equation Eq. (1-5) in the literature includes a term for particle diameter, which is an important factor to consider when trying simulations of powder flow.

The oscillatory shear powder mixer will be used to study the effect of the variation of particle size in the granular material random movement in three dimensions by mixing powders of similar particle size distribution. In addition, the variation in bed expansion (dilation) as a function of particle size will be monitored so that a better understanding of dilatancy phenomena in granular mixing is developed.

4.2 Experimental conditions

Two operating conditions were considered in this study, amplitude of the periodic function and wall velocity. The experimental design method can be seen in Fig. 25. Each circle represents one experiment.

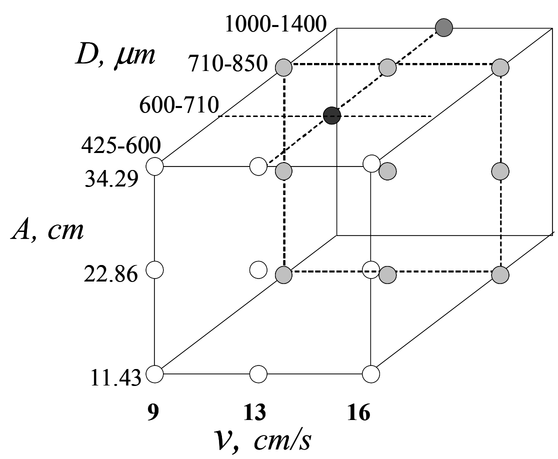

Fig. 25. Scheme of the factors and treatments to analyze the effect of particle size in the mixing

The filling height of the granular material in the cavity was 4.45 cm. The Particle Size Distributions used were in the range of (600-425μm), (710-600μm), (850-710μm) and (1400-1000μm)

Table 4 and Table 5 include the statistics of the particle size of both powders (dark and white). The distribution of particles was narrow enough as to avoid the phenomenon of segregation by particle size.

Table 4. Particle size distribution for blue particles in each range of study

Descriptive Statistics	**(600-425μm)**	**(710-600μm)**	**(850-710μm)**	**(1400-1000μm)**
Mean, μm	566.5	664.45	772.84	1251.68
Median, μm	550.5	663.98	778.00	1255.34
Standard Deviation	94.5	67.23	70.37	153.09
Kurtosis	1.3	0.60	0.44	-0.01
Skewness	0.5	-0.20	-0.10	0.06
Confidence Level	3.3	4.97	5.72	12.76

Table 5. Particle size distribution for white particles in each range of study

Descriptive Statistics	**(600-425μm)**	**(710-600μm)**	**(850-710μm)**	**(1400-1000μm)**
Mean, μm	571.7	655.73	735.63	1240.26
Median, μm	573.4	657.44	740.69	1247.14
Standard Deviation	103.7	87.78	74.20	163.47
Kurtosis	1	0.45	0.26	-0.22
Skewness	-0.3	-0.63	-0.24	-0.20
Confidence Level	4.4	8.62	5.83	16.15

The shape of the particles is considered a strong factor in the variation of particle distribution [113, 114], hence in this study this factor was blocked. Fig. 26 shows a sample of the shape of the particles of each size. They have a regular shape similar for all the sizes. Blue and white particles of each size have a similar surface, thus causing no effect in the results obtained of particle distribution. This particle shapes were neither acicular nor flat as can be seen in Fig. 26, however there is a lot of roughness in the surface supplying enough friction to produce a good transfer of momentum among particles.

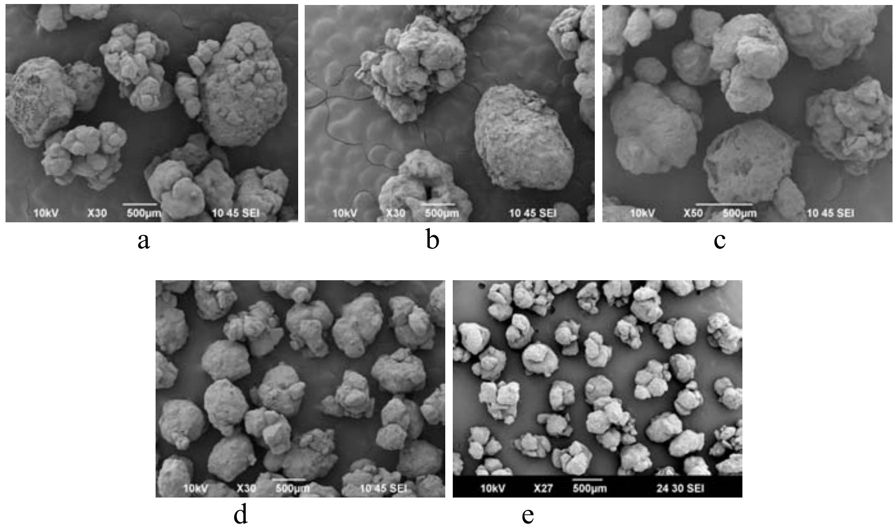

Fig. 26. Shape of particles a) and b) are Blue and White particle respectively (1000 – 1400 μm). c) White particle (710 - 850μm), d) White particle (600 - 710μm). e) White particle (425 - 600μm).

4.3 Results and Discussion

4.3.1 Effect of the particle size on mixing of unrestricted powder at the top surface of the cavity

Fig. 27 shows how the particles were distributed at the surface (x, y) as function of time as motion was applied. As can be seen, larger particle sizes produced faster mixing. In a previous work [86], it was shown that in this system a chaotic convective mixing was produced at the surface due to a discontinuous co-rotational flow. Because of this flow, there is an exponential increase of the interface line between the two powders enhancing the rate of particle interchange of the two zones.

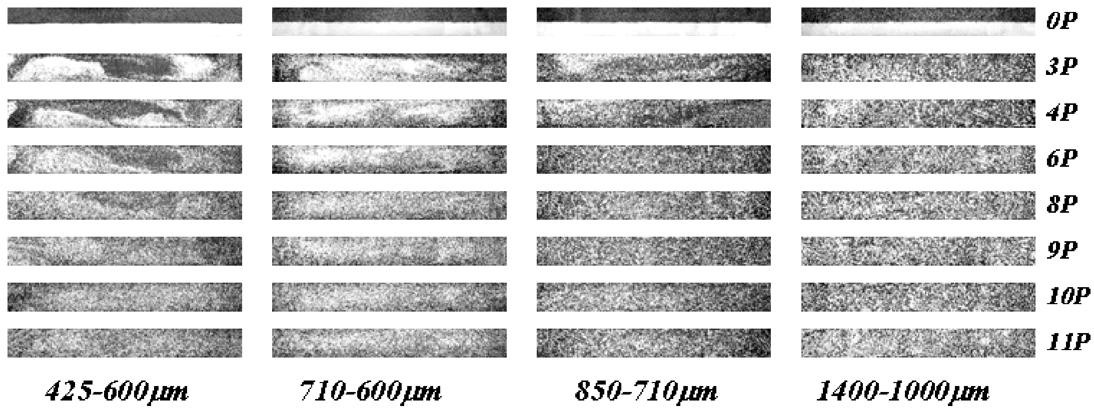

Fig. 27. Variation of mixing in the superficial layer (x,y axis). Effect of time and particle size. *v/W=4.65/s, A=34.29cm*

Since these surfaces were open to the air, the particles experienced zero friction and normal stress from above them allowing the particles to move more freely causing a higher transfer of momentum in this layer. In the case of layers with large particle diameter, the total friction under the particles is lower when compared with small particle diameter [112]. This fact occurs because the total surface area of small particles is higher than the total area of large particles. This smaller frictional area helps larger particles to distribute on the entire surface faster than small ones.

The particles at the surface in contact with the moving walls had the same velocity regardless of the particle size. This behavior was attained due to the high roughness of the mentioned walls, which was constant for all the particle sizes. In addition, particles in the surface did not experience the effect of the weight of other particles, and considering that the particles of all the sizes in this study had similar physical properties including their shape (see, Fig. 26) because they were granulated in the same process with the same operating conditions, the variation in velocity due to particle properties should have been minimum. Hence, the transfer of momentum in the surface from one line of particles to the contiguous line of particles should have happened in the same way for both, large and small particles. Therefore, the reach of movement in the *y* axis away from the moving wall will depend on the particle size [33]. The higher the particle sizes, the larger the y-distance of movement.

For a given depth (y direction) smaller particles moved with lower velocity decreasing the transfer of momentum from its proportional y-distance of movement to the center of the cavity reducing as well the mixing in the surface.

Dilatancy is another factor that affects the motion of particles in the entire cavity, Table 6. The zone of particles near the walls dilated because of the force imparted by the moving walls to the particles. The dilation was maximum near the moving walls and decreased toward the center. It made some particles at the surface in the region of high dilation to move also in the z-direction. The void place was then occupied by particles of the center of the surface that migrated in the direction to the walls. When this migration happened, new particles moved from the layer below the surface in the center of the cavity to fill the place of the migrated particles. This cycle continued helping to produce the profile shown below in Fig. 30. and in [86].

Mixing curves of the surfaces were then generated by plotting the relative standard deviation of the concentration (*RSD*), Eq. (12) (section 3.3.1), as a function of mixing time (Number of cycles), Fig. 28, for each experiment.

It can be seen from Fig. 28 how fast the *RSD* curves reach their asymptotic value called the *RSD* for a random mixture. This is the best mixed state that the mixture can reach randomly and it is calculated as follow [115]:

$$RSD_r = \frac{S_r}{\overline{\overline{C}}} \qquad (15)$$

where

$$S_r = \sqrt{\frac{C_w(1-C_w)}{m}} \qquad (16)$$

Cw is the overall proportion of white particles in the surface when the random mixing is reached and *m* is the number of particles in a sample.

The theoretical *RSDr* value (0.20) for these experiments is reached faster for higher particles and it is not exactly the same for all the sizes because of experimental differences. In addition, the treated particles had small differences in their sizes (see

Table **4** and Table 5), that could have caused segregation in a low scale producing a higher proportion of one of the powders in use at the surface. This small difference in proportion can only be detected by vision systems by means of the intensity of the pixels of the picture. Large scale segregation by density did not happen in these experiments because the difference in density between the two powders was lower than 0.3 g/cm^3 [8].

All the curves in Fig. 28 were plotted beginning in cycle 2 because there is a phenomenon between the initial time and cycle 2 that made the *RSD* to increase or decrease depending on the degree of dilation at the beginning caused by the applied critical shear stress to reach the failure point. In this system, the shear of equilibrium was found quickly but the powders at the surface remained dispersed with different proportion of the initial state during the first cycle. It was noticed that after this cycle the initial proportion was reached and the powders in the surface continue mixing with the pattern shown in Fig. 28.

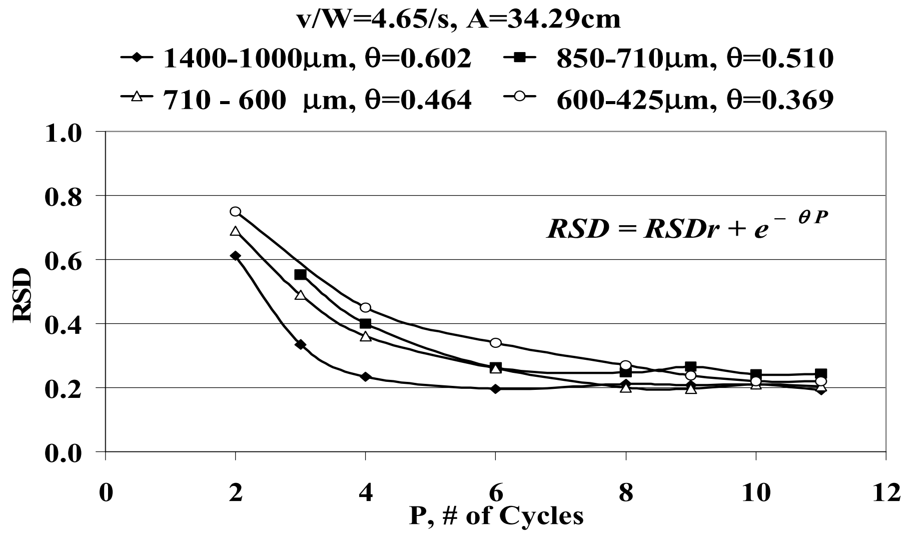

Fig. 28. Mixing rates in the surface as function of time and particle size

Considering the mentioned phenomenon, the *RSD* curves were fitted to the expression, $RSD = RSDr + e^{-\theta P}$, with values of θ increasing as particle size increases as shown in Fig. 29. This figure implies that at higher values of *W/D* the curve will cross the horizontal axis which means that no mixing will occur for certain particle sizes. At lower values of *W/D* the values of theta do not increase substantially meaning that an increase in particle size will not result in a large decrease of mixing times. The exponent θ can be seen as an average Lyapunov exponent and, since it is positive, it says that the time-periodic flow is in general chaotic [103]. Moreover, the higher the particle diameter, the higher the Lyapunov, the more chaotic the dynamics of the system, and the faster the mixing.

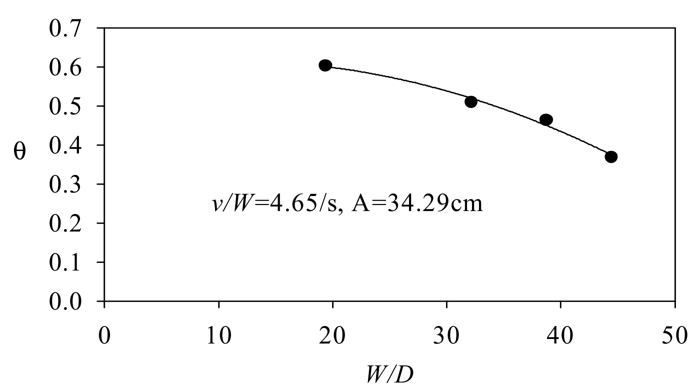

Fig. 29. Variation of the Lyapunov exponent with particle size

4.3.2 Effect of the particle size in the z-axis (height) of the cavity

Fig. 30 demonstrates the effect of the particle size on the mixing profile produced in the height direction of the cavity (plane *y-z*) at the center (*x=L/2*) of the cavity. It shows the distribution of particles moving from the walls (*y=0* and *y=W*) toward the center (*y=W/2*) as shear was applied. As mentioned in section 3.3.2, the triangle at the middle of the cavity is an area of no shear effect and thus no mixing. These triangles are important because they were formed due to the effect of the static wall at bottom where high friction dissipated the shear transferred from the moving walls and thus low mixing was obtained.

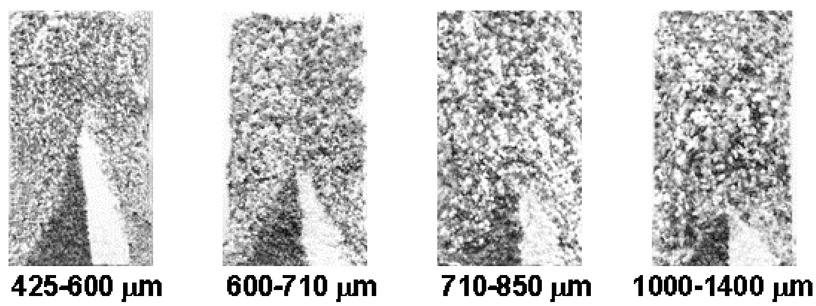

Fig. 30. Distribution of particles in the vertical layer at different particles sizes. ***v/W=4.65/s, A=34.29cm, t=60s***

Fig. 31 shows a summarized description of the behavior shown in Fig. 30. It compares the different triangle heights produced in the plane mentioned above. The term *T-PS#* means triangle formed at the particle size of the number in reference. The wall velocities, amplitude of wall, and filling height were maintained constant for these experiments to study the effect of the particle size in the triangle height and consequently in the mixing.

In Fig. 30, there are two clearly demarked zones separated by a divisor line called slip line. These zones are the mixing zone and the static zone. The static zone (below the slip line) is where the particles did not move, thus they did not mix. The mixing zone, (above the slip line) is the zone of motion, which increased with increases in particle size, lowering the slip line. This expansion in the mixing zone occurred because of a better transfer of momentum from the moving walls to the center and bottom of the cavity.

As it is stated in Fig. 31 the floor of the cavity remained static (highest friction because of the zero velocity and the effect of the weight of the particles), and the top remained opened to the air (lowest friction) [86]. This gradient in friction, together with the dilatancy (higher near the walls and lower in the center) produced a velocity profile in the three axes (*x, y* and *z*) that generated the particle distribution shown in

Fig. **31**. Particles in the compacted zone (center of the cavity) tended to move by diffusion to the dilated zone (toward the top and moving walls).

At the slip line, motion is extremely low because of the high friction offered by the static zone. This friction can be surpassed increasing the particle size as explained below. The density of all the particles (ρ_p) used was the same for every size, see Table 6, which makes that the weight of a vertical arrangement of particles with a specific height is higher for big particles than for small particles, even when there are fewer quantities of big particles in the mentioned arrangement. This effect of higher weight of large particles combined with the fact that the particles of all the sizes in this study had similar physical properties including their shape, caused an increase in the transfer of momentum in the *z* axis toward the bottom in the zone of higher porosity as a consequence of the dilation mentioned before, increasing the diffusion in this direction as well. Therefore, for same operating conditions, large particles have a higher mixing zone and a lower triangle height as well, compared with small particles.

At the intersection between the floor and the moving walls, there is enough transfer of momentum that is able to beat the friction of the static wall producing motion in a small range of distance as shown in Fig. 31. This small range of distance is increased with the increase of particle size because of the increase in transfer of momentum mentioned before.

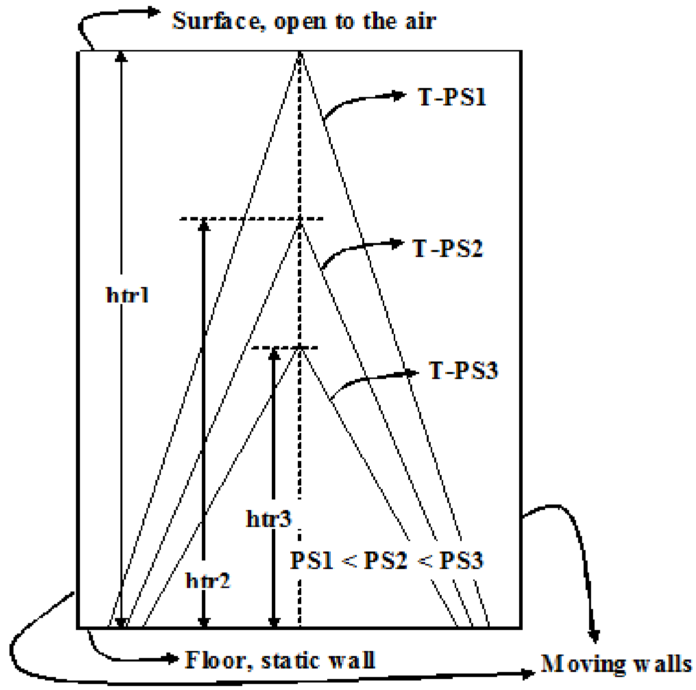

Fig. 31. Diagram of the variation of the location of the slip line as function of particle size

The triangle height will be visible after certain time of mixing when particles over the slip line get more distributed creating a higher contrast in color between the static zone and the mixing zone, therefore it can be tracked by vision systems. The size of the triangle cannot be used to determine the degree of homogeneity of the system but it can be used to determine the highest level of mixing the entire cavity can obtain, which is just when the mixing zone reach the random mixing.

Fig. 32 Fig. 32 shows the behavior of the triangle height for the middle of the cavity depicted in Fig. 30 and Fig. 31 as a function of particle size for a constant filling height of 4.44 cm (horizontal straight line). As can be seen, the triangle height decreased exponentially with increases in particle size. The lower limit of triangle height is because the floor never moves creating a friction that does not allow a possible complete mixing. The limit of the curve to the left is the intersection with the horizontal line representing the height of the powder bed and the lowest particle size that can be mixed by the cavity. Lower particle sizes will create at the surface two zones, a static and a dynamic zone, [33]. Extrapolating both curves in Fig. 32, the particle size would be approximately 400 μm. The maximum y-distance of transfer of momentum for this particle size is then *W/2* or 1.39 cm, which means that the width of the area of movement is approximately 34 particle diameters which differ from the value found by Tardos *et al.*, 2003, [33]. This difference could be caused by many reasons, e.g. roughness of the walls, particles shape, particle distribution, etc.

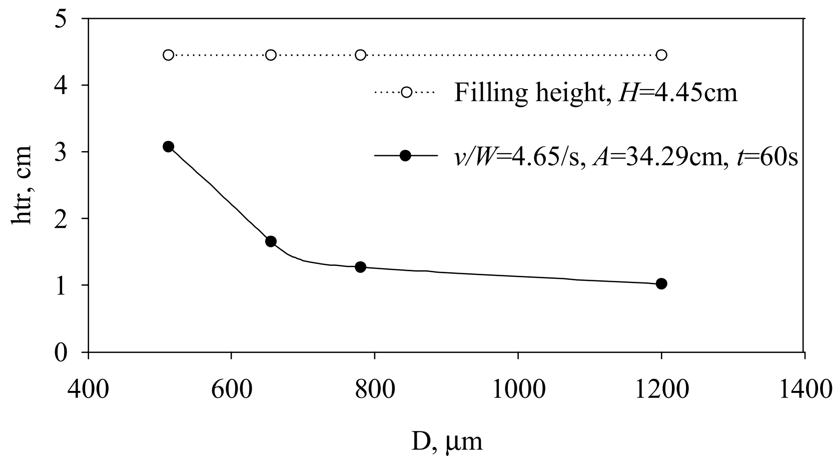

Fig. 32. Tendency of the maximum height of the triangular behavior along the x axis vs Particle diameter

Table 6, presents the relationship of the dilatancy (Δ*H*) with particle size for the white powder. The results for the blue powders were the same even when the difference in density between the two powders was 0.1 g/cm^3. This dilatancy caused enough void fractions among particles and decreased the friction as well as to facilitate the vector movement of particles. It increased in turns the velocity to find the new equilibrium of forces among all the particles when shear forces were applied by the moving walls.

Fig. 33 presents specifically the dilation or expansion of the entire cavity proportionally to the particle diameter. The relationship is described by a slope of $\Delta H/D \cong 4.6$ and a scheme of the phenomena is depicted in Fig. 34. This proportionality increases the effect of the weight to the motion of higher particles to the bottom. The weight of a vertical array of particles increases evidently with an increase of particle size. It indicates that for the moving wall to maintain the same velocity at the different particle sizes, it is necessary to increase the energy transmitted to the walls increasing as well the force applied to particles in the bottom of the cavity in order to maintain the increase in dilation which is proportional to the particle diameter. To maintain the dilation with the mentioned proportionality in diameter, the vertical component of the force applied by the roughness of the wall surfaces has to increase increasing in addition the horizontal component of the force causing a higher transfer of momentum in the y axis along the z axis producing a decrease in the triangle height improving also the total mixing.

Table 6. Results of dilation of white powders in the cavity with a filling height of 5.08 cm and with a resulting volume of 294.97 cm^{3*}.

D (range) *μm*	*D* *mean*	***ΔH*** *cm*	ρ_a *gr/cm^3*	ρ_s *gr/cm^3*	*Vs* *cm^3*	*Vv* *cm^3*	*Ve* *cm^3*	*Vae* *cm^3*	***ΔH/D***
1000 – 1400	1310.26	0.63	0.590	1.4	124.33	170.64	36.58	207.22	4.81
710 – 850	790.63	0.34	0.622	1.4	130.97	164.00	19.74	183.74	4.30
600 – 710	655.73	0.29	0.661	1.4	139.25	155.72	16.84	172.56	4.42
425 – 600	571.70	0.25	0.678	1.4	142.85	152.12	14.52	166.63	4.37

*D : particle size, ΔH : expansion height, ρ_a : density of the bulk of powder in the cavity, ρ_s : density of the powders without void fraction, V_s : volume of the powders without void fraction, V_v : volume occupied by the void fraction at the initial time, V_e : expanded volume, and V_{ae} : total volume of the void fraction when powders are dilated

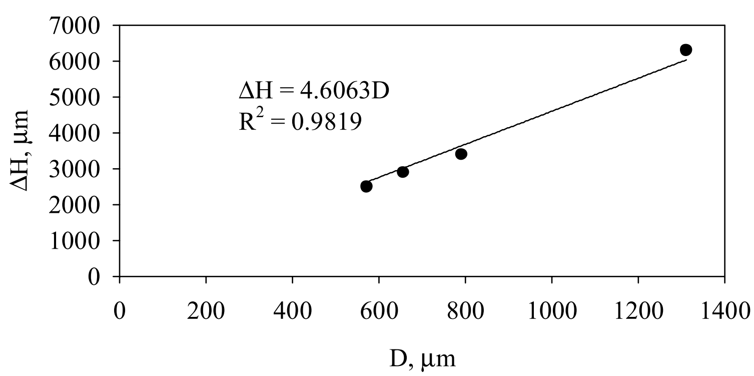

Fig. 33. Relation between the bed expansion of the powders in the cavity vs. the mean particle diameter. ***v/W=4.65/s, A=34.29cm, t=60s***

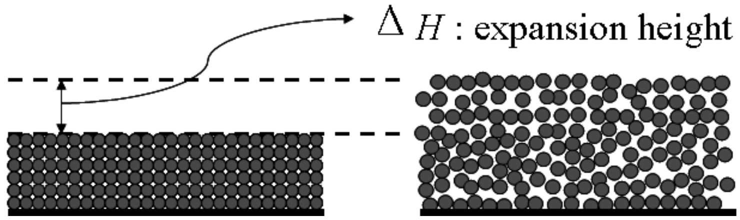

Fig. 34. Scheme of dilation in the depth of the cavity

The triangles in Fig. 30 refer to the powders at the center of the cavity in the *x* axis or lengthier direction, thus the farthest from the vertical static walls. Hence, the discussion mentioned above applies basically to powders that are subjected to shear but were unrestricted to move. Studying the triangle height in the direction from the center to the end static walls, a similar behavior was noticed but the height decreased toward the end static walls.

As explained in Chapter 3, a higher degree of mixing is obtained at the two ends. The more chaotic behavior propagated slowly back to the center of the cavity parallel to the moving walls causing the triangle height to decrease toward the end of the cavity as exposed in Fig. 35 This trend repeated for all wall amplitudes and particle sizes. The tendency can be increased by adding the effect of others factors such as wall velocity and filling height [86]. In the case of wall amplitude, an increase let the particles to be dilated for longer time increasing the effects of dilation mentioned above enhancing the mixing for all the sizes of particles.

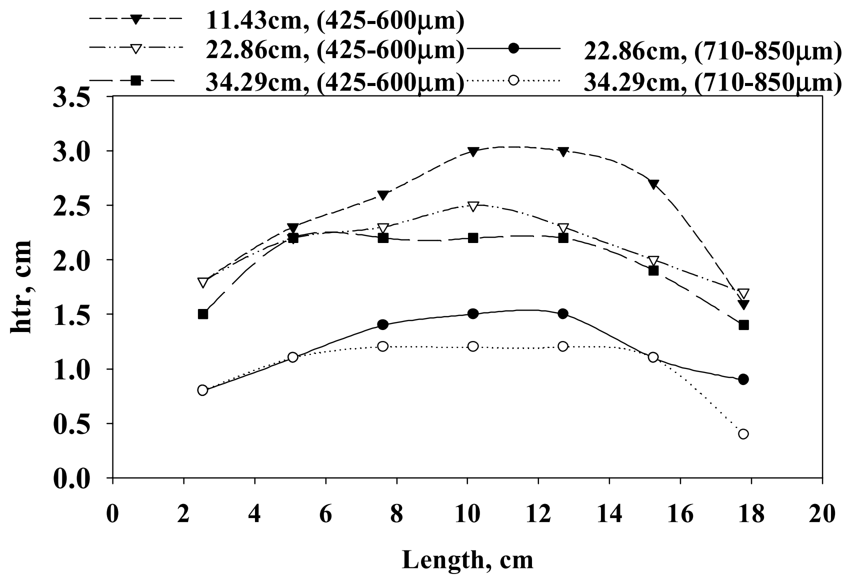

Fig. 35. Effect of the amplitude of the walls and the particle size in the triangle height of the vertical layers. ***v/W=5.73/s, t=60s***

Finally, the mixing extend at the surface is different of that in the z direction. However, there is a relation in their mixing as can be seen in Fig. 27 and Fig. 30 where the faster the mixing in the superficial layer, the lower the height of the triangle. High motion of particles in the surface indicates a lower resistance to the flow meaning that particles under the surface are moving with enough energy to propagate the transfer of motion through the height of the cavity making the zone of no mixing smaller.

4.4 Conclusions

It was confirmed that the small frictional area of large particles helps these particles to distribute on the entire surface faster than the small ones. The theoretical *RSDr* value (0.20) for these experiments is obtained faster for large particles and it is not exactly the same for all the sizes because of experimental error or segregation in a low scale producing a higher proportion of one of the powders in use at the surface.

Because the transfer of momentum at the surface from one line of particles to the contiguous line of particles should have happened in the same way for both, large and small particles, the reach of movement in the *y* axis away from the moving wall will depend on the particle size, therefore the higher the particle sizes, the larger the y-distance of movement. In our case this area of movement is approximately 34 particle diameters. This area is different for different materials because it depends on their physical properties.

In the height direction of the cavity, the large friction occurring in the slip line that cause the no motion of particles, can be beaten increasing the particle size due to the increase of weight of the vertical columns of particles increasing the transfer of momentum in the z and y axes as a consequence of the dilation which was found to be proportional to the particle diameter in the entire cavity as $\Delta H/D \cong 4.6$.

The size of the triangle cannot be used to determine the degree of homogeneity of the system but it can be used to determine the highest level of mixing the entire cavity can obtain, which is just when the mixing zone reaches the random mixing.

5 Effect of Filling Height in Mixing of Granular Materials Under Periodic shear

In the present chapter, the cavity of the oscillatory shear powder mixer will be filled at different heights to obtain a basic knowledge of the effect of the powder weight in the movement in the z axis and in the general mixing of the system as well. Experimental results indicate that the better mixing was obtained when using high initial filling levels. Reasons point out to the weight of the vertical columns of particles and the phenomenon of dilation.

5.1 Introduction

All operational conditions in blenders are considered extremely important because of their direct relation with industrial costs but one of the most important is the filling level because it is directly correlated with the amount of production obtained and the efficiency of mixing processes in the industries. The effect of this factor has been highly studied [17, 21, 106, 116, 117] because of the effect on the behavior of mixing and the end point of mixing (random time of mixing). Nowadays there are certain specific filling level considered when mixing granular material but its essential comprehension is still hindered due to all the transport mechanism involved in a complex realistic three dimensional blender.

This study consisted in designing experiments where the imposed strain rate, particle size distribution, amplitude of moving wall, and time of mixing were maintained constant while varying the initial filling levels in the chamber. The goal was to know the effect of the weight of the granular materials in the mixing in all the zones of the cavity. A physical explanation of the particle motions is given to explain the general mixing behavior.

5.2 Experimental conditions

Two operating conditions were considered in this study, amplitude of the periodic function and wall velocity, each one with only one level, 34.29 cm and 13 cm/s respectively. The Particle Size Distribution used was in the range of (600 – 710 μm) with the same properties as before. Table 7 includes the statistics of the particle size of both powders (dark and white).

Table 7. Particle size distribution (600 - 710 μm)

Descriptive Statistics	Blue particles	White particles
Mean, μm	664.45	655.73
Median, μm	663.98	657.44
Standard Deviation	67.23	87.78
Kurtosis	0.60	0.45
Skewness	-0.20	-0.63
Confidence Level	4.97	8.62

5.3 Results and Discussion

Fig. 36 shows four pictures of the mixing behavior at different initial filling heights. These pictures correspond to the depth of the cavity (plane *y-z*) at the center lengthwise, at *x=L/2.* As explained in section 3.3.2, the floor of the cavity remained static (highest friction because of the zero velocity and the effect of the weight of the particles), and the top remained opened to the air (lowest friction). This gradient in friction, together with the dilatancy (higher near the walls and lower in the center) produced a velocity profile in the three axis (*x, y* and *z*) that generated a particle distribution shown in Fig. 36 causing the formation of a triangle [86].

This figure demonstrates the effect of the filling height on the produced mixing profile showing the distribution of the particles from the moving walls (*y=0* and *y=W*) toward the center ($y=W/2$) as shear was applied. The higher the filling height the lower the triangle height producing a higher mixing degree. This suggests that the weight of the particles induce an increase in the transfer of momentum in the z axis.

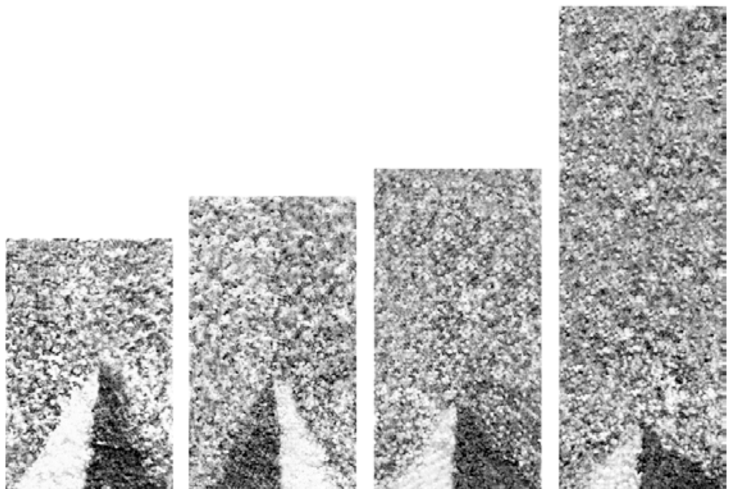

Fig. 36. Distribution of particles in the vertical layer at different filling heights, 3.81, 4.44, 5.08, and 7.62 cm from left to right. *v/W=4.65/s, t=60s, particle size (600-710 μm), Amplitude of wall=34.29 cm.*

In addition to the pictures in Fig. 36, where each picture corresponds to one experiment, 6 additional pictures were taken for each filling height corresponding to different positions along the x axis. Similarly to Fig. 36, the height of the triangles in each picture was measured and plotted in Fig. 37, where the behavior of all the triangle heights along the x axis at different filling heights can be seen.

The straight lines in Fig. 37 refer to the initial filling heights of each experiment and they were connected with their corresponding curve of triangle heights, as depicted by the connector lines, demonstrating that the weight of particles affect the entire cavity volume shown along the x axis of the cavity from the static walls ($x=0$ and $x=L$) to the center of the cavity at $x=L/2$.

As the weight of a vertical column of particles increases with the filling level, increasing at the same time the mixing and reducing the triangle height, so increase the friction of the particles in the bottom with the floor reducing the capacity of the filling height to decrease the static zone linearly. Consequently, if the filling level is increased to a value higher than 3.81 the decrease of the static zone will not be noticeable. This trend is highlighted in Fig. 38 where the tendency of the triangle height of the center of the cavity is depicted with the initial filling level. The straight line corresponds to the initial filling level and the curve below this line corresponds to the triangle height of the center of the cavity. For large values of filling levels, the triangle heights tend to reach an asymptotic value as shown in Fig. 38 corroborating the previous assumption.

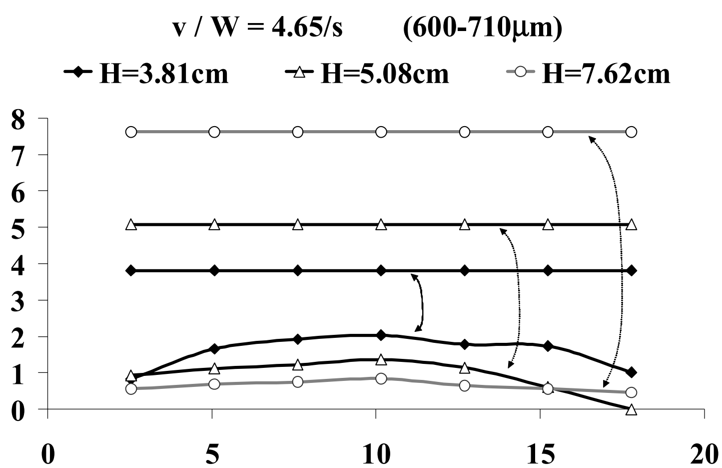

Fig. 37. Effect of the filling height in the triangle height of the vertical layers. *Amplitude of wall = 34.29cm, t=60s.*

At low filling levels, the triangle height tends to have the same height of the filling level indicating that the static zone reaches its maximum height just at the intersection of the two lines. This intersection is the limit of the left side of the curve *htr vs H* at a value of *H* of approximately 2.9 cm.

The continuity of the curve to the left of the intersection point has no physical meaning because there are no triangles anymore in this zone, instead a new shape will be formed that is an isosceles trapezoid indicating that the static zone increases reducing the global mixing. Below the intersection point the surface (layer *x-y*) begin to show static particles just in the center of the surface limiting the movement only to the zone near the moving walls. Therefore, the zone of movement at the surface not only depend on the particle size [33, 118] but also on the filling height.

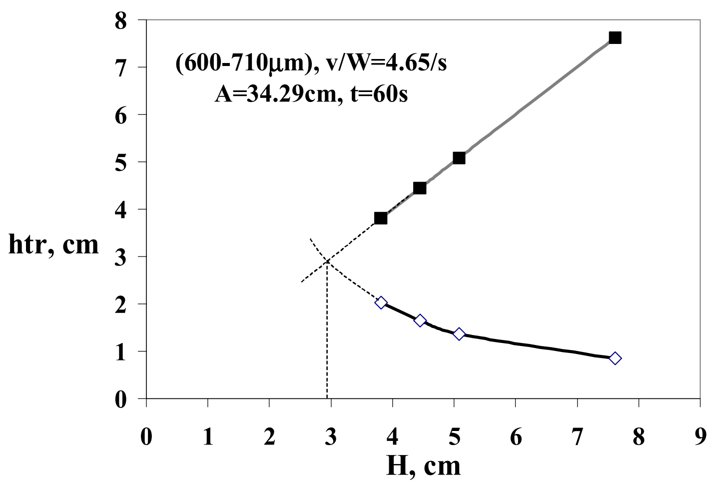

Fig. 38. Trend of the triangle height with the initial filling height

Fig. 39 andFig. 40 show a schematic description of the behavior shown in Fig. 36. They compare the different triangle heights produced in the plane y-z when filling heights is varied. The isosceles trapezoid mentioned before is depicted to give a better understanding of the increasing static zone.

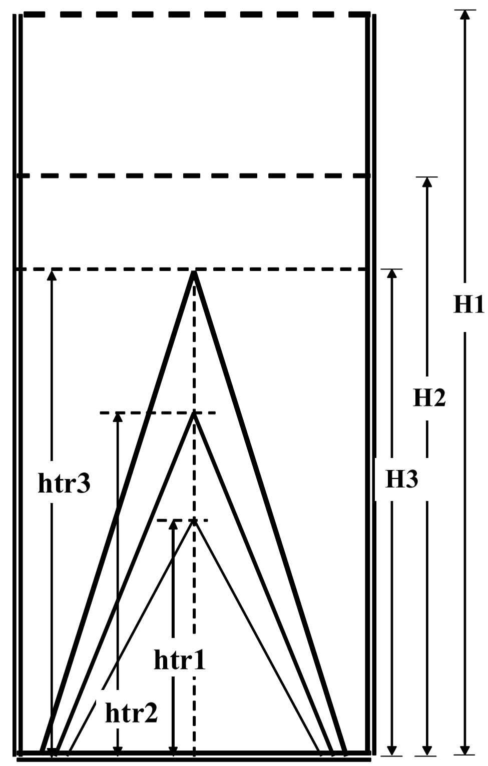

Fig. 39. Diagram of the variation of the location of the slip line as function of filling height

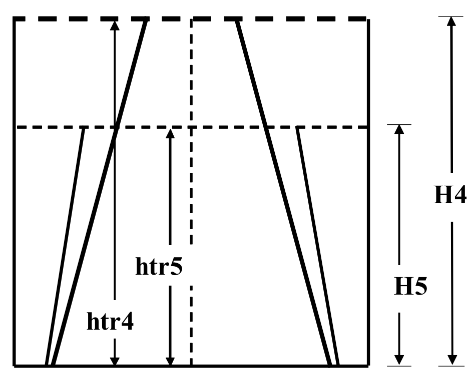

Fig. 40. Scheme of the isosceles trapezoid shape formed when filling level decreases beyond the intersection point shown in Fig. 38.

The gradient in friction between the top and the bottom is different at different filling levels due to the weight of the particles inducing the creation of the profile shown in Fig. 39 and Fig. 40.

The weight of a vertical array of particles increases evidently with an increase on the filling level. As the filling level increases, it is necessary to have an increase in the torque of the shafts applied to the walls Fig. 2 to maintain the constant velocity. This increase in the torque helps to increase the energy transmitted to the walls increasing as well the force applied to particles in the bottom of the cavity in order to maintain the increase in dilation which is proportional to the height of the powder column. The forces imparted by the roughness of the wall surfaces are P and P' for Fig. 41 a and b respectively, having a vertical and horizontal components Pz, Py and Pz', Py'. In order to increase the vertical component to maintain the dilation as mentioned, it is needed to increase the total shear force increasing in addition the horizontal component of the force causing a higher transfer of momentum in the y axis along the z axis producing a decrease in the triangle height and improving the total mixing.

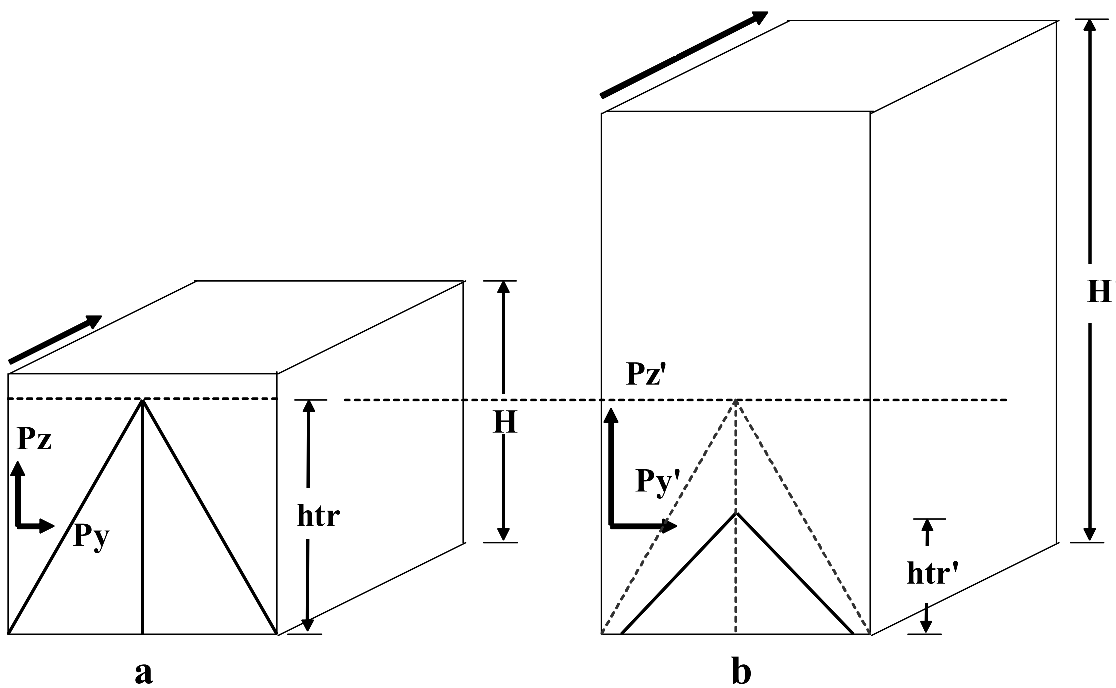

Fig. 41. Scheme of the forces affecting the height of the triangle at two different initial filling heights

5.4 Conclusions

As shear was applied, the effect of increasing the filling level was noticeable decreasing the height of the triangle giving as a result an increase in the mixing due to the increase in the transfer of momentum in the *z* axis.

There is a limit of values of filling heights where values above it will not affect greatly the decrease in triangle height due to the high increase in the friction of the particles with the floor. At low filling levels, the triangle height tends to have the same height of the filling level indicating that the static zone reaches its maximum height producing a new figure in the y-z plane, an isosceles trapezoid.

The trend of the triangle height with the initial filling height reveals that the zone of movement in the surface not only depend on the particle size but also on the filling height.

The weight of the particles is the main factor that affects the trend obtained in the triangle height. The vertical component of the force imparted by the moving walls has to increase to maintain the dilation, increasing as well the horizontal component of the force causing a higher transfer of momentum in the y axis along the z axis producing a decrease in the triangle height and improving the total mixing.

6 FUTURE WORK

- To modify the system to process low scale (smaller) particles and maybe different shapes.
- To modify the system to accommodate even larger filling heights to determine the behavior of the triangle at the filling height tends to infinite.
- To modify the system with the proper sensors to determine the stress field experienced by the powders as they are processed.
- To find correlation among the tendencies of the powder behavior and the properties of the different powders (angle of repose, angle of internal friction, cohesivity, density
- To make simulation of the system using Discrete Element Methods
- To make simulation of the system using continuum constitutive models for cohesionless granular flows

REFERENCES

1. Jain, N., J.M. Ottino, and R.M. Lueptow, *Effect of interstitial fluid on a granular flowing layer.* Journal of Fluid Mechanics, 2004. **508**: p. 23-44.

2. Lagree, P.-Y. and D. Lhuillier, *The Couette flow of dense and fluid-saturated granular media.* European Journal of Mechanics, B/Fluids, 2006. **25**(6): p. 960-970.

3. Baxter, J., et al., *A DEM simulation and experimental strategy for solving fine powder flow problems.* Chemical Engineering Research & Design, 2000. **78**(A7): p. 1019-1025.

4. Khanam, J. and A. Nanda, *Flow of granules through cylindrical hopper.* Powder Technology, 2005. **150**(1): p. 30-35.

5. Laitinen, N., *Opening New Perspectives for Visual Characterisation of Pharmaceutical Solids*, in *Department of Pharmacy*. 2003, University of Helsinki: Helsinki. p. 61.

6. Laurent, B., *Characterisation of wet-mass granulation.* european pharmaceutical review, 2004: p. 95-99.

7. Li, H. and J.J. McCarthy, *Cohesive particle mixing and segregation under shear.* Powder Technology, 2006. **164**(1): p. 58-64.

8. Obregon, L. and C. Velazquez, *Discrimination limit between mean gray values for the prediction of powder concentrations.* Powder Technology, 2007. **175**(1): p. 8-13.

9. Realpe, A. and C. Velazquez, *Image processing and analysis for determination of concentrations of powder mixtures.* Powder Technology, 2003. **134**(3): p. 193-200.

10. Hiseman, M.J.P., et al., *Granular flow in a planetary mixer.* Chemical Engineering Research & Design, 2002. **80**(A5): p. 432-440.

11. Metcalfe, G. and M. Shattuck, *Pattern formation during mixing and segregation of flowing granular materials.* Physica A:, 1996. **233**(3-4): p. 709-717.

12. Cox, G.M. and J.M. Hill, *Some exact mathematical solutions for granular stock piles and granular flow in hoppers.* Mathematics and Mechanics of Solids, 2003. **8**(1): p. 21-50.

13. Kollmann, T. and J. Tomas, *Effect of applied vibration on silo hopper design.* Particulate Science and Technology, 2002. **20**(1): p. 15-31.

14. Zhu, H.P. and A.B. Yu, *Steady-state granular flow in a three-dimensional cylindrical hopper with flat bottom: Microscopic analysis.* Journal of Physics D: Applied Physics, 2004. **37**(10): p. 1497-1508.

15. Jalali, P. and M. Li. *Development of shear bands in annular shear granular flows*. 2003. Boston, MA, United States: Materials Research Society.

16. Elperin, T. and A. Vikhansky, *Granular flow in a rotating cylindrical drum.* Europhysics Letters, 1998. **42**(6): p. 619-623.

17. Arratia, P.E., et al., *A study of the mixing and segregation mechanisms in the Bohle Tote blender via DEM simulations.* Powder Technology, 2006. **164**(1): p. 50-57.

18. Wightman, C. and F.J. Muzzio, *Mixing of granular material in a drum mixer undergoing rotational and rocking motions. I. Uniform particles.* Powder Technology, 1998. **98**(2): p. 113-124.

19. Kuo, H.P., et al., *The influence of DEM simulation parameters on the particle behaviour in a V-mixer.* Chemical Engineering Science, 2002. **57**(17): p. 3621-3638.

20. Zhang, S.B. and V. Sernas, *Incompressible model of solids conveying in a single-screw extruder.* Journal of Reinforced Plastics and Composites, 2002. **21**(15): p. 1399-1409.

21. Sudah, O.S., D. Coffin-Beach, and F.J. Muzzio, *Quantitative characterization of mixing of free-flowing granular material in tote (bin)-blenders.* Powder Technology, 2002. **126**(2): p. 191-200.

22. Jenike, A.W., *Storage and flow of solids.* Utah Eng. Exp. Stn. Bull, 1964. **123**(53): p. 26.

23. Dartevelle, S., *Numerical modeling of geophysical granular flows:1. A comprehensive approach to granular rheologies and geophysical multiphase flows.* Geochemistry Geophysics Geosystems, 2004. **Volume 5**(8): p. 1-28.

24. K.R.Rajagopal and M. Massoudi, *A method for measuring the material moduli of granular materials: Flow in an orthogonal Rheometer.* U.S. Depertment of Energy, 1990. **DE90007160**: p. 28.

25. Nedderman, R.M., *Statics and Kinematics of Granular Materials*. 1992, New York: Cambridge University Press. 372.

26. Tomas, J., *Product design of cohesive powders - Mechanical properties, compression and flow behavior.* Chemical Engineering and Technology, 2004. **27**(6): p. 605-618.

27. Santomaso, A., M. Olivi, and P. Canu, *Mechanisms of mixing of granular materials in drum mixers under rolling regime.* Chemical Engineering Science, 2004. **59**: p. 3269 – 3280.

28. Ottino, J.M. and D.V. Khakhar, *Fundamental research in heaping, mixing, and segregation of granular materials: Challenges and perspectives.* Powder Technology, 2001. **121**(2-3): p. 117-122.

29. Lun, C.K.K., et al., *Kinetic theories for granular flow: inelastic particles in Couette flow and slightly inelastic particles in a general flow field.* Journal of Fluid Mechanics, 1984. **140**: p. 223-256.

30. Gray, D.D. and J.M. Stiles, *On the constitutive relations for frictional flow of granular materials.* , in *Topical Report, U.S. Dept. of Energy DOE/MC/21353-2584, DE88001089*. 1988: Washington, D. C. p. 29.

31. Hopkins, M.A. and M.Y. Louge, *Inelastic microstructure in rapid granular flows of smooth disks.* Phys. Fluids A, 1991. **3**: p. 47-57.

32. Anderson, K.G. and R. Jackson, *A comparison of the solutions of some proposed equations of motion of granular materials for fully developed flow down inclined planes.* Journal of Fluid Mechanic, 1992. **241**: p. 145–168.

33. Tardos, G.I., S. McNamara, and I. Talu, *Slow and intermediate flow of a frictional bulk powder in the Couette geometry.* Powder Technology, 2003. **131**(1): p. 23-39.

34. Castellanos, A., et al., *Flow regimes in fine cohesive powders.* Physical Review Letters, 1999. **82**(6): p. 1156-1159.

35. Tardos, G.I., *A fluid mechanistic approach to slow, frictional flow of powders.* Powder Technology, 1997. **92**(1): p. 61-74.

36. Abu-Zaid, S. and G. Ahmadi, *Analysis of rapid shear flows of granular materials by a kinetic model including frictional losses.* Powder Technology, 1993. **77**(1): p. 7-17.

37. Barbolini, M., et al., *A low cost system for the estimation of concentration and velocity profiles in rapid dry granular flows.* Cold Regions Science and Technology, 2005. **43**(1-2): p. 49-61.

38. Bi, W., et al., *Experimental study of two-dimensional, monodisperse, frictional-collisional granular flows down an inclined chute.* Physics of Fluids, 2006. **18**(12): p. 123302.

39. Goldhirsch, I., *Rapid granular flows.* Annual Review of Fluid Mechanics, 2003. **35**: p. 267-293.

40. Goldhirsch, I. and N. Sela, *Origin of normal stress differences in rapid granular flows.* Physical Review E, 1996. **54**(4): p. 4458-4461.

41. Hui, K., et al., *BOUNDARY CONDITIONS FOR HIGH-SHEAR GRAIN FLOWS.* Journal of Fluid Mechanics, 1984. **145**: p. 223-233.

42. Jalali, P., J. Ritvanen, and P. Sarkomaa, *Transient and steady state behaviors of rapid granular shear flows.* Experiments in Fluids, 2005. **39**(3): p. 552-561.

43. Jalali, P., J. Ritvanen, and P. Sarkomaa, *Stress fluctuations in monodisperse and bidisperse rapid granular shear flows.* Physica A: Statistical Mechanics and its Applications, 2006. **369**(2): p. 535-544.

44. Lavoie, F., L. Cartilier, and R. Thibert, *New methods characterizing avalanche behavior to determine powder flow.* Pharmaceutical Research, 2002. **19**(6): p. 887-893.

45. Louge, M.Y., *Computer-Simulations of Rapid Granular Flows of Spheres Interacting with a Flat, Frictional Boundary.* Physics of Fluids, 1994. **6**(7): p. 2253-2269.

46. Lun, C.K.K., *Kinetic theory for granular flow of dense, slightly inelastic, slightly rough spheres.* Journal of Fluid Mechanics, 1991. **233**: p. 539-559.

47. Ma, D., A.H. Eraslan, and G. Ahmadi, *A Computer Code for Analyzing Transient 3-Dimensional Rapid Granular Flows in Complex Geometries.* Computers & Fluids, 1993. **22**(1): p. 25-50.

48. Massoudi, M. and E.J. Boyle, *A continuum-kinetic theory approach to the rapid flow of granular materials: the effects of volume fraction gradient.* International Journal of Non-Linear Mechanics, 2001. **36**(4): p. 637-648.

49. Shahinpoor, M. and S.P. Lin, *RAPID COUETTE FLOW OF COHESIONLESS GRANULAR MATERIALS.* Acta Mechanica, 1982. **42**(3-4): p. 183-196.

50. Wang, C.-H., R. Jackson, and S. Sundaresan, *Instabilities of fully developed rapid flow of a granular material in a channel.* Journal of Fluid Mechanics, 1997. **342**: p. 179-197.

51. Elaskar, S.A., et al., *A viscoplastic approach to model the flow of granular solids.* International Journal of Solids and Structures, 2000. **37**(15): p. 2185-2214.

52. Massoudi, M. and G. Johnson, *On the flow of a fluid-particle mixture between two rotating cylinders, using the theory of interacting continua.* International Journal of Non-Linear Mechanics, 2000. **35**(6): p. 1045-1058.

53. Herrmann, H.J. and S. Luding, *Modeling granular media on the computer.* Continuum Mechanics and Thermodynamics, 1998. **10**(4): p. 189-231.

54. Mohan, L.S., K. Kesava Rao, and P.R. Nott, *A frictional cosserat model for the slow shearing of granular materials.* Journal of Fluid Mechanics, 2002. **457**: p. 377-409.

55. Massoudi, M., *Constitutive relations for the interaction force in multicomponent particulate flows.* International Journal of Non-Linear Mechanics, 2003. **38**(3): p. 313-336.

56. Massoudi, M., *On the flow of granular materials with variable material properties.* International Journal of Non-Linear Mechanics, 2001. **36**(1): p. 25-37.

57. Massoudi, M., J. Kumar, and C. Lakshmana Rao, *Couette flow of granular materials.* International Journal of Non-Linear Mechanics, 2003. **38**(1): p. 11-20.

58. Schaeffer, D.G., *Instability in the evolution equations describing incompressible granular flow.* J. Differential Equations, 1987(66): p. 19-50.

59. Wang, Z.T. and X.J. Zheng, *Theoretical prediction of creep flux in aeolian sand transport.* Powder Technology, 2004. **139**(2): p. 123-128.

60. Karion, A. and M.L. Hunt, *Wall stresses in granular Couette flows of mono-sized particles and binary mixtures.* Powder Technology, 2000. **109**(1-3): p. 145-163.

61. Mueth, D.M., et al., *Signatures of granular microstructure in dense shear flows.* Nature, 2000. **406**(6794): p. 385-389.

62. Nott, P.R., et al., *The effect of boundaries on the plane Couette flow of granular materials: a bifurcation analysis.* Journal of Fluid Mechanics, 1999. **397**: p. 203-229.

63. Conway, S.L., X. Liu, and B.J. Glasser, *Instability-induced clustering and segregation in high-shear Couette flows of model granular materials.* Chemical Engineering Science, 2006. **61**(19): p. 6404-6423.

64. Alam, M. and P.R. Nott, *Stability of plane Couette flow of a granular material.* Journal of Fluid Mechanics, 1998. **377**: p. 99-136.

65. Lun, C.K.K., *Granular dynamics of inelastic spheres in couette flow.* Physics of Fluids, 1996. **8**(11): p. 2868.

66. Zheng, X.M. and J.H. Hill, *Boundary effects for couette flow of granular materials: Dynamical modelling.* Applied Mathematical Modelling, 1996. **20**(1): p. 82-92.

67. PASSMAN, S.L., J.W. NUNZIATO, and P.B. BAILEY, *Shearing motion of a fluid-saturated granular material.* Journal of Rheology, 1986. **30**(1): p. 167-192.

68. Gudhe, R., K.R. Rajagopal, and M. Massoudi, *Fully developed flow of granular materials down a heated inclined plane.* Acta Mechanica, 1994. **103**: p. 63-78.

69. Campbell, C.S., *Boundary interactions for two-dimensional granular flows. Part 1. Flat boundaries, asymmetric stresses and couple stresses.* . Journal of Fluid Mechanics, 1993. **247**: p. 111-136

70. Hajra, S.K. and D.V. Khakhar, *Radial mixing of granular materials in a rotating cylinder: Experimental determination of particle self-diffusivity.* Physics of Fluids, 2005. **17**(1): p. 013101-013101.

71. Kumara, J., C.L. Rao, and M. Massoudi, *Couette flow of granular materials.* International Journal of Non-Linear Mechanics, 2003. **38**(1): p. 11-20.

72. Cundall, P.A. and O.D.L. Strack, *Discrete numerical model for granular assemblies.* Geotechnique, 1979. **29**(1): p. 47-65.

73. WALTON, O.R. and R.L. BRAUN, *Viscosity, Granular-Temperature, and Stress Calculations for Shearing Assemblies of Inelastic, Frictional Disks.* Journal of Rheology, 1986. **30**(5): p. 949-980.

74. Campbell, C.S. and C.E. Brennen, *Computer Simulation Of Granular Shear Flows.* Journal of Fluid Mechanics, 1985. **151**: p. 167-168.

75. Campbell, C.S., *Stress tensor for simple shear flows of a granular material.* Journal of Fluid Mechanics, 1989. **203**: p. 449-473.

76. Zhou, Y.C., et al., *Rolling friction in the dynamic simulation of sandpile formation.* Physica A: Statistical Mechanics and its Applications, 1999. **269**(2): p. 536-553.

77. Zhou, Y.C., et al., *Microdynamic analysis of the particle flow in a cylindrical bladed mixer.* Chemical Engineering Science, 2004. **59**(6): p. 1343-1364.

78. Lun, C.K.K. and A.A. Bent, *Numerical simulation of inelastic frictional spheres in simple shear flow.* Journal of Fluid Mechanics, 1994. **258**: p. 335-353.

79. Stewart, R.L., et al., *Simulated and measured flow of granules in a bladed mixer - a detailed comparison.* Chemical Engineering Science, 2001. **56**(19): p. 5457-5471.

80. Grasa, G. and J.C. Abanades, *A calibration procedure to obtain solid concentrations from digital images of bulk powders.* Powder Technology, 2001. **114**(1-3): p. 125-128.

81. Bellamy, L., A. Nordon, and D. Littlejohn, *Non-Invasive monitoring of powder mixing with near infrared spectrometry and acoustics.* Spectroscopyeurope, 2004: p. 30-32.

82. Bridgwater, J., S. Forrest, and D.J. Parker, *PEPT for agglomeration?* Powder Technology, 2004. **140**(3): p. 187-193.

83. Lim, S.Y., et al., *Avalanching of granular material in a horizontal slowly rotating cylinder: PEPT studies.* Powder Technology, 2003. **138**(1): p. 25-30.

84. Wildman, R.D., et al., *Investigation of paste flow using positron emission particle tracking.* Powder Technology, 1999. **103**(3): p. 220-229.

85. Wightman, C., F.J. Muzzio, and J. Wilder, *A quantitative image analysis method for characterizing mixtures of granular materials.* Powder Technology, 1996. **89**(2): p. 165-176.

86. Obregón, L., C. Velázquez, and A. Realpe, *Mixing of Granular Materials: Effect of Periodic Shear.* Submitted to Powder Technology, 2008.

87. Alexander, A.W., T. Shinbrot, and F.J. Muzzio, *Granular segregation in the double-cone blender: Transitions and mechanisms.* Physics of Fluids, 2001. **13**(3): p. 578-587.

88. Chester, A.W., et al., *Mixing dynamics in catalyst impregnation in double-cone blenders.* Powder Technology, 1999. **102**(1): p. 85-94.

89. Alexander, A., F.J. Muzzio, and T. Shinbrot, *Segregation patterns in V-blenders.* Chemical Engineering Science, 2003. **58**(2): p. 487-496.

90. Doucet, J., F. Bertrand, and J. Chaouki, *Experimental characterization of the chaotic dynamics of cohesionless particles: Application to a V-blender.* Granular Matter, 2008. **10**(2): p. 133-138.

91. Lemieux, M., et al., *Large-scale numerical investigation of solids mixing in a V-blender using the discrete element method.* Powder Technology, 2008. **181**(2): p. 205-216.

92. Alvarez-Hernandez, M.M., et al., *Practical chaotic mixing.* Chemical Engineering Science, 2002. **57**(17): p. 3749-3753.

93. Laurent, B.F.C., *Scaling factors in granular flow-analysis of experimental and simulations results.* Chemical Engineering Science, 2006. **61**(13): p. 4138-4146.

94. Ottino, J.M. and D.V. Khakhar, *Scaling of granular flow processes: From surface flows to design rules.* Aiche Journal, 2002. **48**(10): p. 2157-2166.

95. Tomas, J., *Assessment of mechanical properties of cohesive particulate solids. Part 2: Powder flow criteria.* Particulate Science and Technology, 2001. **19**(2): p. 111-129.

96. Volfson, D., L.S. Tsimring, and I.S. Aranson, *Partially fluidized shear granular flows: Continuum theory and molecular dynamics simulations.* Physical Review E, 2003. **68**(2 1): p. 021301-1.

97. Chou, C.-S. and M.W. Richman, *Constitutive theory for homogeneous granular shear flows of highly inelastic spheres.* Physica A:, 1998. **259**(3-4): p. 430-448.

98. Daniel, R.C., A.P. Poloski, and A. Eduardo Saez, *A continuum constitutive model for cohesionless granular flows.* Chemical Engineering Science, 2007. **62**(5): p. 1343-1350.

99. Massoudi, M. and T.X. Phuoc, *Numerical solution to the shearing flow of granular materials between two plates.* International Journal of Non-Linear Mechanics, 2005. **40**(1): p. 1-9.

100. Realpe, A., *Modeling of growth kinetics of wet granulation in a high shear mixer by means of image processing and analysis.* PhD Thesis in Chemical Engineering, University of Puerto Rico- Mayagüez campus, 2006: p. 89.

101. Jenike, A.W., *Storage and flow of solids.* Utah Eng. Exp. Stn. Bull., 1964. **123. 53** (26).

102. Venables, H.J. and J.I. Wells, *Powder Mixing.* Drug Development and Industrial Pharmacy, 2001. **27**(7): p. 599–612.

103. Leong, C.W. and J.M. Ottino, *Experiments on mixing due to chaotic advection in a cavity.* Journal of Fluid Mechanics, 1989. **209**: p. 463-499.

104. Zamankhan, P., et al., *Shear-induced particle diffusion in inelastic hard sphere fluids.* Physical Review E. Statistical Physics, Plasmas, Fluids, and Related Interdisciplinary Topics, 1998. **58**(5-A): p. 5237-5240.

105. Boyle, E.J. and M. Massoudi, *Theory for granular materials exhibiting normal stress effects based on Enskog's dense gas theory.* International Journal of Engineering Science, 1990. **28**(12): p. 1261-1275.

106. Ottino, J.M. and D.V. Khakhar, *Mixing and segregation of granular materials.* Annual Review of Fluid Mechanics, 2000. **32**: p. 55-91.

107. Cisar, S.E., P.B. Umbanhowar, and J.M. Ottino, *Radial granular segregation under chaotic flow in two-dimensional tumblers.* Physical Review E - Statistical, Nonlinear, and Soft Matter Physics, 2006. **74**(5): p. 051305.

108. Liu, X., M. Metzger, and B.J. Glasser, *Couette flow with a bidisperse particle mixture.* Physics of Fluids, 2007. **19**(7): p. 073301.

109. Yang, S.C., *Density effect on mixing and segregation processes in a vibrated binary granular mixture.* Powder Technology, 2006. **164**(2): p. 65-74.

110. Chaudhuri, B., et al., *Cohesive effects in powder mixing in a tumbling blender.* Powder Technology, 2006. **165**(2): p. 105-114.

111. Alexander, A., F.J. Muzzio, and T. Shinbrot, *Effects of scale and inertia on granular banding segregation.* Granular Matter, 2004. **5**(4): p. 171-175.

112. Iordanoff, I., K. Elkholy, and M.M. Khonsari, *Effect of particle size dispersion on granular lubrication regimes.* Proceedings of the Institution of Mechanical Engineers, Part J: Journal of Engineering Tribology, 2008. **222**(6): p. 725-739.

113. Cleary, P.W., *The effect of particle shape on simple shear flows.* Powder Technology, 2008. **179**(3): p. 144-163.

114. Pena, A.A., R. Garcia-Rojo, and H.J. Herrmann, *Influence of particle shape on sheared dense granular media.* Granular Matter, 2007. **9**(3-4): p. 279-291.

115. Lacey, P.M.C., *The mixing of solid particles.* Chem. Age, Lond., 1945. **119**(145): p. 53-59.

116. Boateng, A.A. and P.V. Barr, *Granular flow behaviour in the transverse plane of a partially filled rotating cylinder.* Journal of Engineering and Applied Science, 1997. **330**: p. 233-249.

117. Khakhar, D.V., et al., *Transverse flow and mixing of granular materials in a rotating cylinder.* Physics of Fluids, 1997. **9**(1): p. 31.

118. Obregon, L., C. Velazquez, and A. Realpe, *Effect of Particle Size in Mixing of Granular Materials Under Periodic shear.* To be Submitted to Powder Technology, 2009.

119. Montgomery, D.C., *Design and Analysis of Experiments*. 5th ed. 2001, Arizona, USA: John Wiley and Sons Inc.

Appendix A. Image Analysis

The resolutions of the images were 3888 x 2592 pixels for a total approximately of 10 MP. All the images were acquired in color, RGB 32-bit, and then digitized to be converted to 8-bit gray color by means of the image acquisition board using the software IMAQ Vision 6.0 for LabView 6i (National Instrument). In the new format, there are 256 intensities of gray values, beginning in cero (Black color) and ending in 255 (White color).

The matrix of pixels of each picture was sent to excel software using macros. Each matrix was reduced to a new resolution that had the same number of particles of each picture. This reduction was done averaging all the intensities of gray values of the pixels corresponding to a single particle and then repeating the same process for all the particles in the picture.

Now we have pictures with new resolution and intensities of gray values. So that we could differentiate particles of different colors, a histogram of number of pixels vs. intensity value of each pixel was plotted as shown in Fig. 42. There are two curves that correspond to each powder. The curve on the left relates to the dark powder (blue powder) and the curve in the right correspond to white powder. The corresponding intensity value on the limit of separation between the curves was taken.

Then, it was proceeded to convert all the values lower than the intensity value of the limit of separation to *1*. The rest of the values were converted to *0* in order to work with binary numbers to make easier the mixing study.

Finally, a new array of number is obtained, see Fig. 43a. This new array is separated in different sectors, Fig. 43b, in order to calculate relative standard deviation of the concentration of one powder with respect to the other with Eq. (12). The number of sectors is calculated with characteristic operation curves, [119].

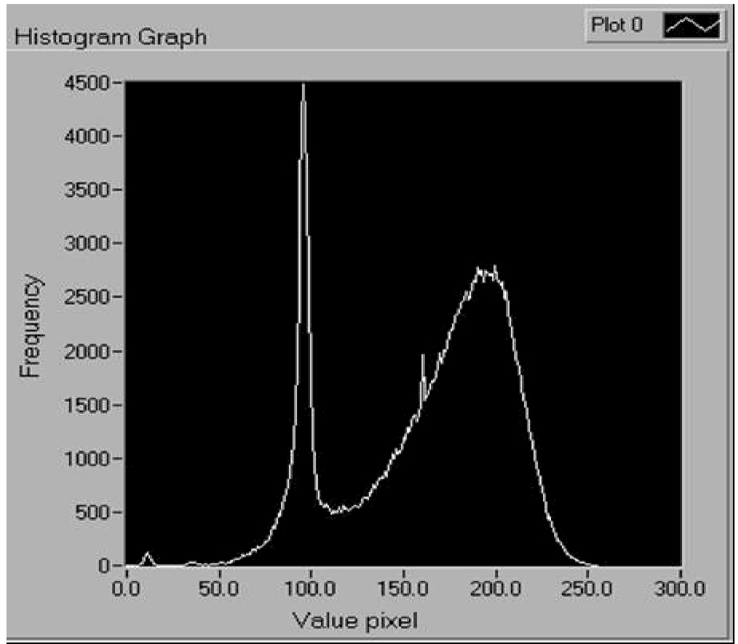

Fig. 42. Pixel histogram of a gray image of a mixture of blue powder with white powder

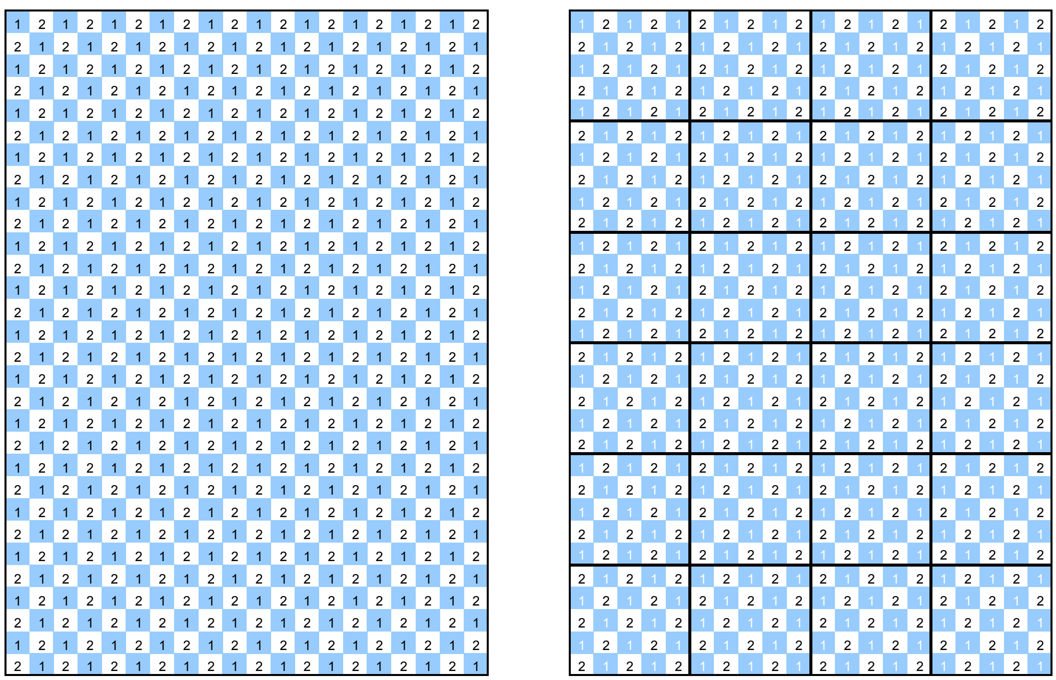

Fig. 43. (a). Schematic picture of a sample where blue powder is mixed homogeneously with white powder and each powder represented by one number. (b) Sample divided by equal sized sectors.

Appendix B. Dilation Measurement

With a hard paper of low density a figure with a triangle shape was constructed, see Fig. 44. This triangle had a base with the dimensions of the base of the cavity and had a top where a ruler made with the same material of paper was installed. When an experiment was ready to run, this object was placed on the surface of the powders in the cavity. When motion was applied to the system, an expansion of the entire volume appears and was measured with the ruler installed on the top of the object with a high speed camera. The weight of this triangular object was so small, approximately 1g, that the normal force applied to the powders in the top was negligible. This experiment was run at different particle size and the results shown in Fig. 33.

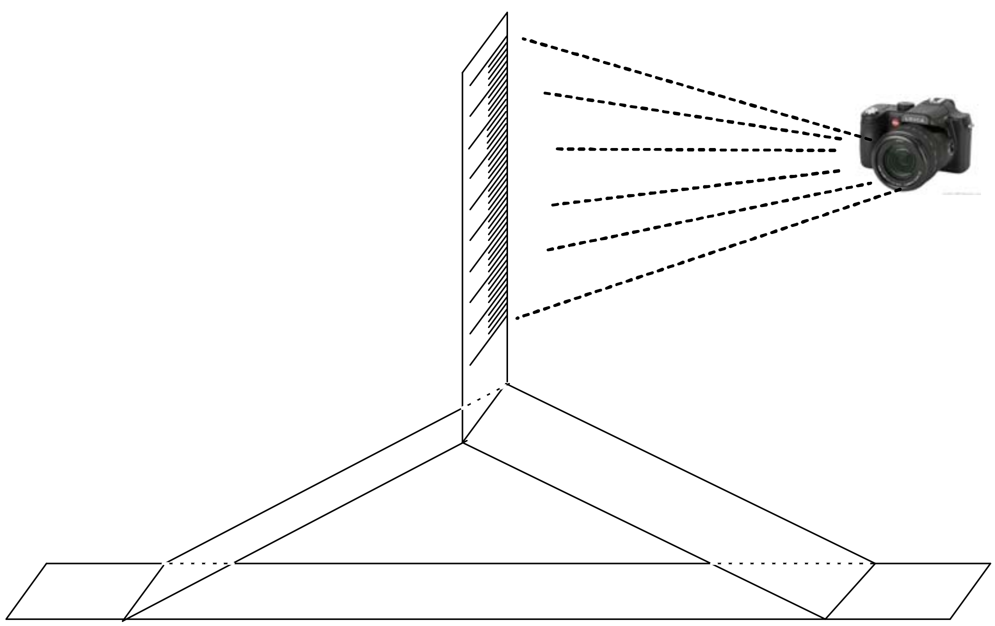

Fig. 44. Sketch of the triangular object that measure dilation